Inorganic Chemistry

Article

pubs.acs.org/IC

Ruthenium Bis-diimine Complexes with a Chelating Thioether Ligand: Delineating 1,10-Phenanthrolinyl and 2,2′-Bipyridyl Ligand Substituent Effects

Nathir A. F. Al-Rawashdeh,[‡] Sayandev Chatterjee,[§] Jeanette A. Krause,[†] and William B. Connick*,[†]

[†]Department of Chemistry, University of Cincinnati, P.O. Box 210172, Cincinnati, Ohio 45221-0172, United States

[‡]Department of Applied Chemical Sciences, Jordan University of Science & Technology, P.O. Box 3030, Irbid-22110, Jordan

[§]Energy and Environment Directorate, Pacific Northwest National Laboratory, Richland, Washington 99354, United States

Supporting Information

ABSTRACT: Despite the high π-acidity of thioether donors, ruthenium(II) complexes with a bidentate 1,2-bis(phenylthio)-ethane (dpte) ligand and two chelating diimine ligands (i.e., $Ru(diimine)_2(dpte)^{2+}$) exhibit room-temperature fluid solution emission originating from a lowest MLCT excited state (diimine = 2,2′-bipyridine, 5,5′-dimethyl-2,2′-bipyridine 4,4′-di-*tert*-butyl-2,2′-bipyridine, 1,10-phenanthroline, 5-methyl-1,10-phenanthroline, 5-chloro-1,10-phenanthroline, 5-bromo-1,10-phenanthroline, 5-nitro-1,10-phenanthroline, 4,7-diphenyl-1,10-phenanthroline, and 3,4,7,8-tetramethyl-1,10-phenanthroline). Crystal structures show that the complexes form 2 of the 12 possible conformational/configurational isomers, as well as nonstatistical distributions of geometric isomers; there also are short intramolecular $\pi-\pi$ interactions between the diimine ligands and dpte phenyl groups. The photoinduced solvolysis product, $[Ru(diimine)_2(CH_3CN)_2](PF_6)_2$, for one complex in acetonitrile also was characterized by single-crystal X-ray diffraction. Variations in the MLCT energies and Ru(III/II) redox couple, $E^{\circ\prime}(Ru^{3+/2+})$, can be understood in terms of the influence of the donor properties of the ligands on the mainly metal-based HOMO and mainly diimine ligand-based LUMO. $E^{\circ\prime}(Ru^{3+/2+})$ also is quantitatively described using a summative Hammett parameter (σ_T), as well as using Lever's electrochemical parameters (E_L). Recommended parametrizations for substituted 2,2′-bipyridyl and 1,10-phenanthrolinyl ligands were derived from analysis of correlations of $E^{\circ\prime}(Ru^{3+/2+})$ for 99 homo- and heteroleptic ruthenium(II) tris-diimine complexes. This analysis reveals that variations in $E^{\circ\prime}(Ru^{3+/2+})$ due to substituents at the 4- and 4′-positions of bipyridyl ligands and 4- and 7-positions of phenanthrolinyl ligands are significantly more strongly correlated with σ_p^+ than either σ_m or σ_p. Substituents at the 5- and 6-positions of phenanthrolinyl ligands are best described by σ_m and have effects comparable to those of substituents at the 3- and 8-positions. Correlations of E_L with σ_T for 1,10-phenanthrolinyl and 2,2′-bipyridyl ligands show similar results, except that σ_p and σ_p^+ are almost equally effective in describing the influence of substituents at the 4- and 4′-positions of bipyridyl ligands. MLCT energies and d^5/d^6-electron redox couples of the complexes with 5-substituted 1,10-phenanthroline exhibit correlations with values for other d^6-electron metal complexes that can be rationalized in terms of the relative number of diimine ligands and substituents.

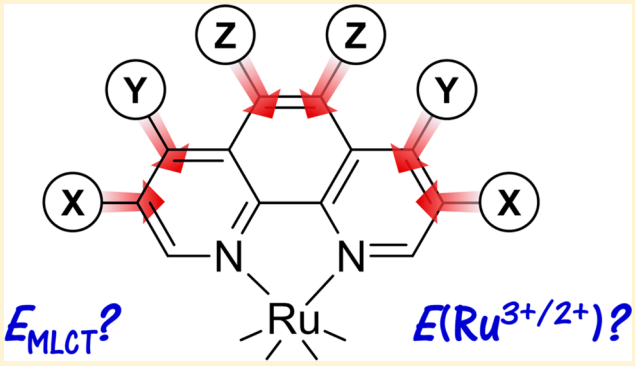

INTRODUCTION

This report describes the structural, spectroscopic, and electrochemical properties of a series of ruthenium(II) complexes with a bidentate 1,2-bis(phenylthio)ethane (dpte) ligand and two substituted 2,2′-bipyridyl or 1,10-phenanthrolinyl ligands. These observations and assembled literature data are leveraged to delineate empirical relationships between spectroscopic and electrochemical data, as well as parameters describing diimine ligand substituents. The work was motivated by the fact that ruthenium(II) complexes having at least one polypyridyl ligand are potentially useful in applications such as dye-sensitized solar cells, photocatalysis, sensing, displays, and biotechnology.[1−4] These complexes typically have a mainly metal-centered HOMO and a diimine-centered LUMO. This situation results in low-lying MLCT states, as well as metal- and ligand-based electron-transfer chemistry. Features include good chemical stability, high light absorptivity in the visible region, relatively long-lived lowest excited states, reversible electron-transfer reactions, and rich photochemistry. Despite growing knowledge of these properties, the development of reliable guidelines for designing complexes that meet specific and demanding performance criteria remains a challenge.

Received: September 3, 2013
Published: December 10, 2013

   dx.doi.org/10.1021/ic4022454 | *Inorg. Chem.* 2014, 53, 294−307

Investigations of a large number of such complexes have been indispensable in improving the understanding of how ligand donor properties modulate redox chemistry and characteristics of MLCT states. For example, within certain series of complexes, it has been found that the MLCT absorption and emission energies are correlated with ΔE, defined as the difference between the mainly metal-based $Ru^{3+/2+}$ couple and the first diimine ligand-based redox couple.[5−22] Similar correlations have been noted for luminescent osmium(II), rhenium(I), and platinum(II) complexes.[5,18,23−27] Relationships involving externally derived parameters also are potentially useful for predicting properties of unknown compounds. For example, linear free energy relationships between the metal-based $Ru^{3+/2+}$ couple and diimine ligand pK_a values,[28] as well as the free ligand reduction potentials,[29] have been reported. There also is growing interest in correlations between experimental data and calculated parameters.[30,31] One of the most common strategies has been to identify correlations of redox and spectroscopic properties with Hammett parameters for substituents on nonchromophoric ligands,[8,32−36] as well as chromophoric ligands, such as 2,2′;6′,2″-terpyridyl[20] and 2,2′-bipyridyl ligands.[37−41] However, such studies have focused on rather narrow sets of complexes. In the case of redox potentials, the success of such treatments implies the existence of electrochemical ligand additivity relationships,[42,43] which have been expanded upon by Lever[44] to produce a powerful set of ligand electrochemical parameters (E_L).[39,45,46] Whereas some attention has been given to the influence of 2,2′-bipyridyl ligand substituents on the properties of ruthenium(II) complexes,[15,28−30,37−41,47−51] comparatively little attention has been given to the systematization of 1,10-phenanthrolinyl ligand substituent effects on the properties of ruthenium(II) polypyridyl complexes.[33,52−56] However, there have been several investigations of other luminescent transition-metal systems.[23,24,26,53,54,57−59]

Against this backdrop, we were interested in expanding knowledge of the chemistry of divalent ruthenium 1,10-phenanthrolinyl complexes with alkyl and aryl thioether ligands.[60] The high π-acidity of thioether ligands is expected to destabilize MLCT states, and therefore, emission from such complexes is reasonably anticipated to be susceptible to quenching by low-lying, thermally accessible ligand-field states. In support of this supposition, we note that ruthenium(II) 2,2′-bipyridyl complexes with a chelating dialkyl thioether ligand and two N-donor pyridyl or benzimidazolyl ligands exhibit very short-lived MLCT emissions (τ < 100 ns).[21,22] Similarly, Collin et al. reported that $Ru(phen)_2(dpte)^{2+}$ undergoes rather efficient photosubstitution reactions.[61] Building on our earlier studies of $Ru(diimine)(dpte)_2^{2+}$ complexes,[62] we report here the synthesis and characterization of a new series of $Ru(diimine)_2(dpte)^{2+}$ complexes. These compounds exhibit surprisingly long-lived emission from a lowest MLCT state. The redox potentials and spectroscopic properties can be understood in terms of the relative σ- and π-donor properties of the ligands. Moreover, these observations have inspired a broad investigation of 2,2′-bipyridyl and 1,10-phenanthrolinyl substituent effects. That analysis has yielded surprising insight into the electronic influence of phenanthrolinyl ligand substituents, including those at the 5- and 6-positions. Thus, we report here a set of recommended summative Hammett parametrizations for 2,2′-bipyridyl and 1,10-phenanthrolinyl ligands, as well as estimates of E_L for 56 diimine ligands and dpte.

EXPERIMENTAL SECTION

General. $RuCl_3·3H_2O$ was obtained from Pressure Chemical (Pittsburgh, PA). 5-Methyl-1,10-phenanthroline (CH_3phen) and 5-chloro-1,10-phenanthroline (Clphen) were obtained from Alfa Aesar (Ward Hill, MA). 5,5′-Dimethyl-2,2′-bipyridine (dmbpy) and 4,4′-di-*tert*-butyl-2,2′-bipyridine (dbbpy) were obtained from Aldrich Chemical Co. (Milwaukee, WI). 5-Nitro-1,10-phenanthroline (NO_2phen), 1,10-phenanthroline (phen), 4,7-diphenyl-1,10-phenanthroline (dpphen), and 3,4,7,8-tetramethyl-1,10-phenanthroline (tmphen) were obtained from Acros (Somerville, NJ). 5-Bromo-1,10-phenanthroline (Brphen)[63] and 1,2-bis(phenylthio)ethane[64] were synthesized as previously described. Tetra-*n*-butylammonium hexafluorophosphate ($TBAPF_6$) was prepared according to a literature procedure,[65] recrystallized at least twice from methanol and dried under vacuum prior to use. Acetonitrile for emission and electronic absorption spectroscopic studies was distilled from calcium hydride. Deuterated acetonitrile and acetone were obtained from Cambridge Isotope Laboratories (Andover, MA). Acetonitrile for electrochemical studies was obtained from Burdick and Jackson (Muskegon, MI).

Methods. Elemental analyses were performed by Atlantic Microlab, Inc. (Norcross, GA). ^{1}H NMR spectra were recorded at room temperature using a Bruker AMX 400 MHz wide-bore spectrometer and referenced vs the characteristic solvent resonance. Mass spectra were obtained by electrospray ionization of acetonitrile solutions using a Micromass Q-TOF-2 instrument. UV−visible absorption spectra were recorded using a HP8453 Diode Array spectrometer; data are summarized in Table 3 and Table S2 (Supporting Information). Emission spectra were recorded using a SPEX Fluorolog-3 Fluorimeter equipped with a double emission monochromator and a single excitation monochromator. Samples were typically excited near the MLCT absorption maximum where concentrations had been adjusted to give absorbances of 0.1−0.25. Emission spectra were corrected for instrumental response. Samples were subjected to a minimum of three freeze−pump−thaw cycles prior to lifetime measurements using 410−440 nm light from a Continuum Panther optical parametric oscillator pumped with the third harmonic of a Continuum Surelite II Nd:YAG laser. Emission transients were detected using a modified PMT connected to a Tektronix TDS580D oscilloscope and modeled using in-house software on a Microsoft Excel Platform. Cyclic voltammetry measurements were carried out using a standard three-electrode cell and a 100 B/W electrochemical workstation from Bioanalytical Systems. Scans were recorded on samples dissolved in 0.1 M $TBAPF_6$ acetonitrile solution using a Pt wire auxiliary electrode, and a 3.0 mm diameter glassy-carbon working electrode. The electrode potential was referenced vs Ag/AgCl (3.0 M NaCl). Under these conditions, the ferrocene/ferrocenium couple occurred at 0.435 V with an anodic−cathodic peak potential separation (ΔE_p) of 59 mV at 0.1 V s^{-1}. The potentials were standardized to the normal hydrogen electrode (NHE) by addition of 0.195 V (=0.630−0.435).[66] For reversible and quasi-reversible processes, the value of $(E_{pc} + E_{pa})/2$ at 0.1 V/s, an approximation of the formal potential for a redox couple, is referred to as $E^{\circ\prime}$.

Chemometric Analyses. Data analyses were carried out with Microsoft Excel and Mathematica 8.0 using conventional statistical treatments.[67,68] The Pearson product-moment correlation coefficient (R) ranges from −1 to 1 and is referred to as the correlation coefficient. The significance level in hypothesis testing was 5% (α = 0.05). Parametric statistical treatment of such data must be accepted with caution because of uncertainties concerning underlying assumptions of normality, independence, homogeneity of variances, and the validity of the model, as well as uncertainties in Hammett parameters (σ). In the case of $E^{\circ\prime}(Ru^{3+/2+})$ values, primary literature work was located using SciFinder and in references cited by Juris et al.[69] and Lever.[44] The resulting 199 redox potential measurements on 99 complexes are listed in Table S3 in the Supporting Information. We use "measurement" to indicate a single report of a redox potential for a given complex. Thus, there may be multiple measurements per complex. Measurements were required to meet several criteria for inclusion. With the exception of complexes having one dpte ligand

dx.doi.org/10.1021/ic4022454 | Inorg. Chem. 2014, 53, 294−307

(Table S4, Supporting Information), data were restricted to homo- and heteroleptic $Ru(X)(Y)(Z)^{2+}$ complexes in which X, Y, and Z are 2,2′-bipyridyl and/or 1,10-phenanthrolinyl ligands. Each complex was required to exhibit a reversible (or nearly so) $Ru^{3+/2+}$ redox couple in acetonitrile solution with 0.1 M electrolyte. We excluded complexes with bipyridyl ligands having non-hydrogen substituents at the 6- or 6′-positions and those with phenanthrolinyl ligands having substituents at the 2- or 9-positions. Substituents were required to have so-called "preferred values" of the σ_m, σ_p, and σ_p^+ designated in the compendium by Hansch, Leo, and Hoekman (see Table S5, Supporting Information).[70] (Exploration of other substituent parameters proved impractical because well-determined values are not available.) Data were retained only if there were no obvious errors and the method of referencing the electrochemical potentials to a reference electrode was considered unambiguous. The data are representative, but not intended to be exhaustive. Some characteristics of the data are summarized in Table S6 (Supporting Information). All 199 measurements were used in determination of ligand electrochemical parameters (E_L). For correlations with Hammett parameters, replicate measurements of $E^{\circ\prime}(Ru^{3+/2+})$ were averaged. The complexes were divided into three data sets: **A**, **B**, and **C** (Tables S7−S9, Supporting Information). $Ru(4,4'\text{-}(NEt_2)_2\text{-bpy})_3^{2+}$ (4,4′-$(NEt_2)_2$-bpy = 4,4′-diethylamino-2,2′-bpy) was excluded from Hammett correlations because of conflicting reports of $E^{\circ\prime}(Ru^{3+/2+})$ and the high leverage of these data. $Ru((PhCH{=}CH)_2\text{-bpy})_3^{2+}$ ($(PhCH{=}CH)_2$-bpy = 4,4′-bis(2-phenylethenyl)-2,2′-bipyridine)[37] was an extreme outlier under all parametrizations using σ_p^+ to describe 4,4′-substituents, which raises doubts about σ_p^+ for this substituent and/or the value of $E^{\circ\prime}(Ru^{3+/2+})$. Therefore, this complex also was omitted from Hammett correlations, including those involving E_L.

Potentials were referenced to NHE (or SHE) following the electrode conversions suggested by Pavlishchuk and Addison.[66] Potentials reported against the saturated Ag/AgCl and Ag/AgCl (3 M NaCl) reference electrodes were referenced to NHE by addition of 0.198 and 0.209 V, respectively.[71,72] It may be useful to point out that some authors have reported the expected potentials of ruthenium complexes in water vs NHE based on values determined in acetonitrile, by noting that the $Ru(bpy)_3^{3+/2+}$ couple in acetonitrile vs SCE has the same value in water vs NHE and with the assumption that this is true of related complexes.[73] Such potentials were converted to values in acetonitrile vs NHE by addition of 0.25 V.

More than two-thirds of the replicates are for $Ru(bpy)_3^{2+}$ ($N = 44$), $Ru(4,4'\text{-dimethyl-2,2'-bpy})_3^{2+}$ ($N = 16$), and $Ru(phen)_3^{2+}$ ($N = 10$). In each case, the standard deviation (σ) of the mean redox potential exceeds typical estimates of experimental error: $Ru(bpy)_3^{2+}$, 1.52(3) V; $Ru(4,4'\text{-dimethyl-2,2'-bipyridine})_3^{2+}$, 1.37(3) V; $Ru(phen)_3^{2+}$, 1.52(5) V. In the case of $Ru(phen)_3^{2+}$, discarding the two worst outliers gives 1.53(2) V. Sources of disagreement in potentials have previously been outlined,[44] and these include variations in electrolyte/electrode, corrections for junction potentials and IR drop, solvent purity, reference electrodes, and reference electrode conversions, as well as nonstatistical fluctuations such as outliers.

***cis*-RuL_2Cl_2 (L = phen, CH_3phen, NO_2phen, Clphen, Brphen, tmphen, dpphen, dmbpy, or dbbpy).** The complexes were prepared by modification of the procedure for the synthesis of *cis*-$Ru(bpy)_2Cl_2{\cdot}2H_2O$ (bpy = 2,2′-bipyridine).[74,75] In a typical reaction, $RuCl_3{\cdot}3H_2O$ (7.84 g, 30 mmol), 2,2′-bipyridine (9.36 g, 60 mmol), and LiCl (0.85 g, 20 mmol) were refluxed in dimethylformamide (60 mL) for 6 h under argon with vigorous stirring. After allowing the mixture to cool to room temperature, HPLC grade acetone (150 mL) was added, and the resultant solution was cooled at −25 °C overnight. Filtering the resulting mixture yielded a red to red-violet filtrate and a nearly black microcrystalline product. The solid was washed well with several portions of cold water (∼75 mL), followed by several portions of diethyl ether (∼75 mL). The solid was dried by suction. Yields were typically 70−75%. The products were characterized by ^{1}H NMR spectroscopy and mass spectrometry.

$[Ru(phen)_2(dpte)](PF_6)_2$ (1). Drawing on the work from Root et al. for the preparation of bis(2,2′-bipyridine)(thioether)ruthenium(II) hexafluorophosphate complexes ($[(bpy)_2Ru(SS)](PF_6)_2$),[60] *cis*-$Ru(phen)_2Cl_2{\cdot}2H_2O$ (0.566 g, 1 mmol) and a 5-fold excess of dpte (1.23 g, 5 mmol) were refluxed in a 1:1 mixture of distilled water and ethanol (100 mL) under argon for 4 h with vigorous stirring. The dark red-violet reaction mixture gradually became a yellow-orange solution. After the resulting solution was cooled to room temperature, excess dpte ligand was removed by extraction with diethyl ether. Excess NH_4PF_6 was added to the yellow-orange solution to induce precipitation. The resulting yellow powder was collected by filtration and washed with cold water (75 mL) and diethyl ether (75 mL), before being dried in vacuo. Yield: 0.6036 g, 60%. Analytical samples were obtained either by direct crystallization from acetone−ether at ∼0 °C or by column chromatography on activated neutral alumina (2:1 and 1:1 benzene:CH_3CN), followed by recrystallization from acetone−ether. Recovered yields varied between 50 and 70%. ^{1}H NMR (CD_3CN, δ): 9.94 (d, 2H, $J = 5.2$ Hz; H_2), 8.66 (d, 2H, $J = 6.8$ Hz; H_4), 8.40 (d, 2H, $J = 6.8$ Hz; H_7), 8.20 (dd, 2H, $J = 5.2$ Hz, $J = 3.6$ Hz; H_3), 8.00 (d, 2H, $J = 6.8$ Hz; H_9), 7.85 (d, 2H, $J = 6.8$ Hz; H_5), 7.51 (dd, 2H, $J = 5.2$ Hz, $J = 5.2$ Hz; H_6), 7.33 (d, 2H, $J = 3.6$ Hz; H_8), 6.78 (dd, 2H, $J = 7.2$ Hz, $J = 7.6$ Hz; H_p), 6.47 (dd, 4H, $J = 7.6$ Hz, $J = 8.0$ Hz; H_m), 6.19 (d, 4H, $J = 7.6$ Hz; H_o), 3.88 (d, 2H, $J = 8.4$ Hz; CH_2), 3.20 (d, 2H, $J = 8.4$ Hz; CH_2). MS-ESI (m/z): 852.9 ($[Ru(phen)_2(dpte)](PF_6)^+$), 351.9 ($Ru(phen)_2(dpte)^{2+}$). Anal. Calcd. For $RuC_{38}H_{30}N_4S_2P_2F_{12}$: C, 45.70; H, 3.03; N, 5.62. Found: C, 45.51; H, 3.01; N, 5.38.

$[Ru(CH_3phen)_2(dpte)](PF_6)_2$ (2). The product was isolated as a yellow powder by following the synthetic procedure for **1** and substituting *cis*-$Ru(CH_3phen)_2Cl_2{\cdot}2H_2O$ (0.298 g, 0.5 mmol) for *cis*-$Ru(phen)_2Cl_2{\cdot}2H_2O$. Yield 0.38 g, 74%. ^{1}H NMR (CD_3CN, δ): 9.93 (d, 1H, $J = 4.4$ Hz), 9.84 (d, 1H, $J = 2.4$ Hz), 8.73 (d, 1H, $J = 8.4$ Hz), 8.51 (dd, 2H, $J = 8.4$ Hz, $J = 8.0$ Hz), 8.29 (d, 1H, $J = 8.0$ Hz), 8.21 (d, 1H, $J = 4.8$ Hz), 8.15 (d, 1H, $J = 4.8$ Hz), 7.98 (d, 1H, $J = 4$ Hz), 7.88 (d, 1H, $J = 4.4$ Hz), 7.77 (s, 1H), 7.73 (s, 1H), 7.54 (dd, 1H, $J = 4.8$ Hz, $J = 5.6$ Hz), 7.47 (dd, 1H, $J = 5.2$ Hz, $J = 5.2$ Hz), 6.80 (dd, 2H, $J = 7.2$ Hz, $J = 6.4$ Hz; H_p), 6.48 (t, 4H, $J = 7.2$ Hz; H_m), 6.15 (d, 4H, $J = 6.4$ Hz; H_o), 3.86 (d, 2H, $J = 8.0$ Hz; CH_2), 3.18 (d, 2H, $J = 8.0$ Hz; CH_2), 2.77 (s, 3H; CH_3), 2.71 (s, 3H, CH_3). MS-ESI (m/z): 880.8 ($[Ru(CH_3phen)_2(dpte)](PF_6)^+$), 366.4 ($Ru(CH_3phen)_2(dpte)^{2+}$). Anal. Calcd. For $RuC_{40}H_{34}N_4S_2P_2F_{12}$: C, 46.83; H, 3.34; N, 5.46. Found: C, 46.56; H, 3.41; N, 5.59.

$[Ru(Clphen)_2(dpte)](PF_6)_2$ (3). The product was isolated as an orange powder by following the synthetic procedure for **1** and substituting *cis*-$Ru(Clphen)_2Cl_2{\cdot}2H_2O$ (0.319 g, 0.5 mmol) for *cis*-$Ru(phen)_2Cl_2{\cdot}2H_2O$. Yield 0.37 g, 70%. ^{1}H NMR (CD_3CN, δ): 10.0 (d, 1H, $J = 4.8$ Hz), 9.95 (d, 1H, $J = 4.8$ Hz), 8.91 (d, 1H, $J = 8.0$ Hz), 8.67 (d, 1H, $J = 8.4$ Hz), 8.60 (d, 1H, $J = 8.4$ Hz), 8.36 (d, 1H, $J = 8$ Hz), 8.31 (dd, 1H, $J = 7.6$ Hz, $J = 5.6$ Hz), 8.22 (dd, 1H, $J = 7.2$ Hz, $J = 5.6$ Hz), 8.16 (s, 1H), 8.12 (s, 1H), 8.06 (d, 1H, $J = 4.8$ Hz), 7.98 (d, 1H, $J = 4.4$ Hz), 7.64 (d, 1H, $J = 3.6$ Hz), 7.55 (d, 1H, $J = 2.8$ Hz), 6.87 (t, 2H, $J = 7.2$ Hz; H_p), 6.53 (t, 4H, $J = 7.6$ Hz; H_m), 6.19 (d, 4H, $J = 6.8$ Hz; H_o), 3.89 (d, 2H, $J = 7.6$ Hz; CH_2), 3.19 (d, 2H, $J = 7.6$ Hz; CH_2). MS-ESI (m/z): 920.9 ($[Ru(Clphen)_2(dpte)](PF_6)^+$); 386.8 ($Ru(Clphen)_2(dpte)^{2+}$). Anal. Calcd. For $RuC_{38}H_{28}Cl_2N_4S_2P_2F_{12}$: C, 42.79; H, 2.67; N, 5.25. Found: C, 42.65; H, 2.67; N, 5.44.

$[Ru(Brphen)_2(dpte)](PF_6)_2$ (4). The product was isolated as a dark-yellow powder by following the synthetic procedure for **1** and substituting *cis*-$Ru(Brphen)_2Cl_2{\cdot}2H_2O$ (0.363 g, 0.5 mmol) for *cis*-$Ru(phen)_2Cl_2{\cdot}2H_2O$. Yield 0.346 g, 60%. ^{1}H NMR (CD_3CN, δ): 9.94 (d, 2H, $J = 3.6$ Hz), 8.66 (d, 2H, $J = 8.4$ Hz), 8.40 (d, 2H, $J = 7.6$ Hz), 8.21 (s, 2H), 7.97−7.91 (m, 4H), 7.52 (d, 2H, $J = 4.8$ Hz), 6.78 (t, 2H, $J = 7$ Hz; H_p), 6.47 (dd, 4H, $J = 7.2$ Hz, $J = 7.6$ Hz; H_m), 6.19 (d, 4H, $J = 7.2$ Hz; H_o), 3.88 (d, 2H, $J = 8.0$ Hz; CH_2), 3.20 (d, 2H, $J = 8.0$ Hz; CH_2). Anal. Calcd. For $RuC_{38}H_{28}Br_2N_4S_2PF_6$: C, 45.16; H, 2.79; N, 5.54. Found: C, 45.36; H, 3.03; N, 5.56.

$[Ru(NO_2phen)_2(dpte)](PF_6)_2$ (5). The product was isolated as a light-brown material by following the procedure for **1** and substituting *cis*-$Ru(NO_2phen)_2Cl_2{\cdot}2H_2O$ (0.53 g, 0.8 mmol) for *cis*-$Ru(phen)_2Cl_2{\cdot}2H_2O$. Yield 0.66 g, 76%. ^{1}H NMR (CD_3CN, δ): 10.08 (d, 2H, $J = 4$ Hz), 9.14 (d, 2H, $J = 8.8$ Hz), 8.93 (d, 1H, $J = 8.4$ Hz), 8.87 (s, 1H), 8.82 (s, 1H), 8.63 (d, 1H, $J = 8$ Hz), 8.36 (m, 2H), 8.16 (dd, 2H, $J = 3.2$ Hz, $J = 4.8$ Hz), 7.68 (m, 2H), 6.86 (t, 2H, $J = 7.6$ Hz; H_p), 6.54

dx.doi.org/10.1021/ic4022454 | Inorg. Chem. 2014, 53, 294−307

Table 1. Crystallographic Data Summary for $[Ru(CH_3phen)_2(dpte)](PF_6)_2 \cdot 0.5Et_2O$ (2·0.5Et$_2$O), $[Ru(NO_2phen)_2(dpte)](PF_6)_2 \cdot 4/3CH_3CN$ (5·4/3CH$_3$CN), $[Ru(dpphen)_2(dpte)](PF_6)_2 \cdot 2CH_3CN$ (7·2CH$_3$CN), $[Ru(dbbpy)_2(dpte)](PF_6)_2 \cdot CH_3CN$ (9·CH$_3$CN), and $[Ru(5,5'\text{-dmbpy})_2(CH_3CN)_2](PF_6)_2$ (8P)

	2·0.5Et$_2$O	5·4/3CH$_3$CN	7·2CH$_3$CN	9·CH$_3$CN	8P
formula	$2\{[C_{40}H_{34}N_4S_2Ru](PF_6)_2\} \cdot C_3H_6O$	$[C_{38}H_{28}N_6O_4S_2Ru](PF_6)_2 \cdot 4/3CH_3CN$	$[C_{62}H_{46}N_4S_2Ru](PF_6)_2 \cdot 2CH_3CN$	$[C_{50}H_{62}N_4S_2Ru](PF_6)_2 \cdot CH_3CN$	$[C_{28}H_{30}N_6Ru](PF_6)_2$
M_r	2109.76	1143.12	1384.27	1215.22	841.59
T (K)	150(2)	193(2)	150(2)	193(2)	150(2)
λ (Å)	0.77490	0.77490	1.54178	0.77490	0.77490
crystal syst	monoclinic	monoclinic	monoclinic	monoclinic	monoclinic
space group	*Cc*	*C*2/*c*	*C*2/*c*	*C*2/*c*	*C*2/*c*
crystal color/habit	yellow rod	dark red rod	yellow rod	yellow block	orange block
crystal size, mm	0.11 × 0.03 × 0.02	0.04 × 0.02 × 0.02	0.17 × 0.06 × 0.03	0.05 × 0.04 × 0.04	0.07 × 0.06 × 0.03
θ range, deg	2.62−29.02	2.55−27.12	2.92−67.87	2.38−31.12	2.40−31.16
a, Å	18.8314(17)	25.961(2)	32.5431(10)	29.518(2)	25.396(3)
b, Å	21.5487(17)	9.2613(8)	8.7643(3)	9.9121(7)	10.4086(11)
c, Å	21.0387(18)	19.6949(16)	23.0088(8)	20.8271(14)	15.790(2)
α, deg	90	90	90	90	90
β, deg	90.317(2)	100.194(2)	111.525(2)	108.383(2)	127.756(3)
γ, deg	90	90	90	90	90
V (Å^3), Z	8537.2(13), 4	4660.6(7), 4	6104.8(4), 4	5782.7(7), 4	3299.9(7), 4
μ, mm^{-1}	0.787	0.739	3.943	0.593	0.836
ρ_{calcd} g cm^{-3}	1.641	1.629	1.506	1.396	1.694
no. reflns collecd	47 545	18 991	18 510	35 813	20 863
no. unique. reflns/R_{int}	17493/0.0579	3950/0.0473	5291/0.0345	7176/0.0446	4108/0.0748
max/min transmission	0.9844/0.9184	0.9854/0.9746	0.8909/0.5537	0.9767/0.9710	0.9754/0.9438
R_1/wR_2 [$I > 2\sigma(I)$][a]	0.0463/0.1047	0.0624/0.1704	0.0435/0.1070	0.0406/0.1130	0.0449/0.1167
R_1/wR_2 (all data)[a]	0.0616/0.1121	0.0654/0.1721	0.0505/0.1107	0.0453/0.1163	0.0542/0.1242

[a] $R_1 = \sum||F_o| - |F_c||/\sum|F_o||$, $wR_2 = [\sum w(F_o^2 - F_c^2)^2/\sum w(F_o^2)^2]^{1/2}$.

dx.doi.org/10.1021/ic4022454 | Inorg. Chem. 2014, 53, 294−307

(dd, 4H, J = 8 Hz, J = 7.6 Hz; H_m), 6.21 (d, 4H, J = 6.8 Hz; H_o), 3.91 (d, 2H, J = 8 Hz; CH_2), 3.19 (d, 2H, J = 8 Hz; CH_2). MS-ESI (m/z): 943.1 ($[Ru(NO_2phen)_2(dpte)](PF_6)^+$), 395.8 ($Ru(NO_2phen)_2(dpte)^{2+}$). Anal. Calcd. For $RuC_{38}H_{28}N_6O_4S_2P_2F_{12}$: C, 41.96; H, 2.59; N, 7.73. Found: C, 41.76; H, 2.59; N, 8.21.

$[Ru(tmphen)_2(dpte)](PF_6)_2$ (6). The product was isolated as an orange powder by following the procedure for **1** and substituting *cis*-$Ru(tmphen)_2Cl_2{\cdot}2H_2O$ (0.34 g, 0.5 mmol) for *cis*-$Ru(phen)_2Cl_2{\cdot}2H_2O$. Yield 0.435 g, 78%. ^1H NMR (CD_3CN, δ): 9.52 (s, 2H), 8.06 (d, 4H, J = 3.6 Hz), 7.66 (s, 2H), 6.77 (dd, 2H, J = 6.4 Hz, J = 7.2 Hz; H_p), 6.46 (t, 4H, J = 7.6 Hz; H_m), 6.16 (d, 4H, J = 7.6 Hz; H_o), 3.81 (d, 2H, J = 8.0 Hz; CH_2), 3.18 (d, 2H, J = 8.0 Hz; CH_2), 2.87 (s, 6H, p-CH_3), 2.82 (s, 6H, p-CH_3), 2.66 (s, 6H, m-CH_3), 2.55 (s, 6H, m-CH_3). MS-ESI (m/z): 964.9 ($[Ru(tmphen)_2(dpte)](PF_6)^+$), 408.4 ($Ru(tmphen)_2(dpte)^{2+}$). Anal. Calcd. For $RuC_{46}H_{46}N_4S_2P_2F_{12} + H_2O$: C, 48.98; H, 4.29; N, 4.97. Found: C, 48.94; H, 4.15; N, 5.07.

$[Ru(dpphen)_2(dpte)](PF_6)_2$ (7). The product was isolated as a yellow powder by following the procedure for **1** and substituting *cis*-$Ru(dpphen)_2Cl_2{\cdot}2H_2O$ (0.436 g, 0.5 mmol) for *cis*-$Ru(phen)_2Cl_2{\cdot}2H_2O$. Yield 0.31 g, 61%. ^1H NMR (CD_3CN, δ): 10.02 (d, 2H, J = 6 Hz), 8.21 (dd, 4H, J = 5.6 Hz, J = 5.6 Hz), 7.90 (d, 4H, J = 7.2 Hz), 7.78–7.73 (m, 10H), 7.63–7.61 (m, 6H), 7.56 (d, 2H, J = 5.6 Hz), 7.51 (dd, 4H, J = 4 Hz, J = 2 Hz), 6.94 (t, 2H, J = 7.2 Hz; H_p), 6.63 (dd, 4H, J = 8.4 Hz, J = 7.2 Hz; H_m), 6.39 (d, 4H, J = 7.6 Hz; H_o), 3.97 (d, 2H, J = 8.0 Hz; CH_2), 3.30 (d, 2H, J = 8.0 Hz; CH_2). MS-ESI (m/z): 1157.2 ($[Ru(dpphen)_2(dpte)](PF_6)^+$), 504.5 ($[Ru(dpphen)_2(dpte)]^{2+}$). Anal. Calcd. For $RuC_{62}H_{46}N_4S_2P_2F_{12}$: C, 57.19; H, 3.56; N, 4.30. Found: C, 57.25; H, 3.55; N, 4.29.

$[Ru(dmbpy)_2(dpte)](PF_6)_2$ (8). The product was isolated as a yellow-orange powder by following the procedure for **1** and substituting *cis*-$Ru(dmbpy)_2Cl_2{\cdot}2H_2O$ (0.288 g, 0.5 mmol) for *cis*-$Ru(phen)_2Cl_2{\cdot}2H_2O$. Yield 0.385 g, 77%. ^1H NMR (CD_3CN, δ): 9.29 (s, 2H), 7.83 (d, 2H, J = 7.6 Hz), 7.76 (d, 2H, J = 8.4 Hz), 7.72 (d, 2H, J = 8 Hz), 7.68 (d, 2H, J = 8.4 Hz), 7.44 (s, 2H), 7.23 (t, 2H, J = 7.6 Hz; H_p), 6.91 (dd, 4H, J = 7.2 Hz, J = 7.6 Hz; H_m), 6.46 (d, 4H, J = 7.6 Hz; H_o), 3.84 (d, 2H, J = 8 Hz; CH_2), 3.08 (d, 2H, J = 8 Hz CH_2), 2.66 (s, 12H; CH_3). MS-ESI (m/z): 861.0 ($[Ru(dmbpy)_2(dpte)](PF_6)^+$), 356.6 ($Ru(dmbpy)_2(dpte)^{2+}$). Anal. Calcd. For $RuC_{38}H_{38}N_4S_2P_2F_{12}$: C, 45.37; H, 3.81; N, 5.57. Found: C, 45.01; H, 3.81; N, 5.59.

$[Ru(dbbpy)_2(dpte)](PF_6)_2$ (9). The product was isolated as a yellow-orange powder by following the procedure for **1** and substituting *cis*-$(dbbpy)_2RuCl_2{\cdot}2H_2O$ (0.744 g, 1 mmol) for *cis*-$Ru(phen)_2Cl_2{\cdot}2H_2O$. Yield 0.938 g, 80%. ^1H NMR (CD_3CN, δ): 9.39 (broad-s, 1H), 8.83 (broad-s, 1H), 7.92 (d, 2H, J = 11 Hz), 7.81 (broad-s, 1H), 7.61 (d, 2H, J = 4.8 Hz), 7.51 (broad-s, 1H), 7.31 (d, 2H, J = 6.4 Hz), 7.33 (dd, 2H, J = 7.6 Hz, J = 7.2 Hz), 7.11 (dd, 2H, J = 6.8 Hz, J = 7.6 Hz; H_p), 6.87 (dd, 4H, J = 7.2 Hz, J = 7.6 Hz; H_m), 6.40 (d, 4H, J = 7.6 Hz; H_o), 3.83 (d, 2H, J = 6 Hz; CH_2), 3.02 (d, 2H, J = 6 Hz; CH_2), 1.98 (s, 36H; CH_3). Anal. Calcd. For $RuC_{50}H_{62}N_4S_2P_2F_{12} + H_2O$: C, 50.37; H, 5.41; N, 4.70. Found: C, 50.36; H, 5.18; N, 4.33.

X-ray Crystallography.[76] Crystals of **2**·0.5Et_2O grew as yellow rods from ethanol–acetone–ether. Diffusion of diethyl ether into acetonitrile solutions yielded **5**·4/3CH_3CN, **7**·2CH_3CN, and **9**·CH_3CN as dark red crystals, yellow rods, and yellow blocks, respectively. Attempts to grow crystals of **8** in room light following a similar procedure resulted in yellow blocks of $[Ru(dmbpy)_2(CH_3CN)_2](PF_6)_2$ (**8P**) in which the dpte ligand of **8** was replaced with two acetonitrile ligands. CCDC deposit numbers: 948678 (**2**·0.5Et_2O), 948679 (**5**·4/3CH_3CN), 948680 (**7**·2CH_3CN), 948681 (**9**·CH_3CN), and 948682 (**8P**).

For X-ray examination and data collection, a suitable crystal was mounted in a loop with paratone-N and transferred immediately to the goniostat bathed in a cold stream. Low-temperature intensity data for **2**·0.5Et_2O (150 K) and **8P** (150 K) were collected with a Bruker APEXII CCD detector, whereas data for **5**·4/3CH_3CN (150K) and **9**·CH_3CN (193K) were collected with a Bruker Platinum200 detector at Beamline 11.3.1 at the Advanced Light Source (Lawrence Berkeley National Laboratory). Synchrotron radiation was tuned to λ = 0.77490 Å. Data for **7**·2CH_3CN (150 K) were collected using a Bruker SMART6000 CCD diffractometer using graphite-monochromated Cu Kα radiation (λ = 1.54178 Å). Data were collected at 0.3° intervals of ω with a maximum 2θ value of ~60° for the synchrotron data and ~135° for Cu. All data frames were processed using SAINT and corrected for absorption and beam corrections based on the multiscan technique (SADABS). The structures were solved by a combination of direct methods using SIR2004 or SHELXTL, expanded using the difference Fourier technique and refined by full-matrix least-squares on F^2. Non-hydrogen atoms were refined with anisotropic displacement parameters with the exception of select disordered F atoms. Typical disorder is observed for the PF_6^- counterions; where possible, a multicomponent disorder model for the F atoms is given. H-atom positions were calculated and treated with a riding model. Isotropic displacement parameters were defined as a^*U_{eq} of the adjacent atom (a = 1.5 for methyl and 1.2 for all others). The refinements converged with crystallographic agreement factors summarized in Table 1.

2·0.5Et_2O crystallizes as two independent molecules, A and B. One of the methyl substituents in molecule B is disordered over two positions, bonding to C63B and C64B (occupancy set at 50:50). The NO_2 group in **5**·4/3CH_3CN is disordered over two sites, bonded to either C13 (67% occupancy) or C14 (33%). CH_3CN (67% occupancy) resides in the vacancy when NO_2 is not present at C14. Additionally, the NO_2 group itself is disordered, a reasonable disorder model is given for the N3A/N3B group. However, disorder on the N3C group remains unresolved. Several bond and displacement parameter constraints were applied to regularize the geometry of the disordered NO_2 groups. In **9**·CH_3CN, one of the *t*-butyl groups is disordered. A two-component disorder model is included. The occupancy of the C atoms was refined (88%); the minor component anisotropic displacement parameter was set equivalent to the major component. A bond restraint also was applied to the C26–C28B bond so that its bond distance is similar to those of the remaining bonds about C26. A disordered CH_3CN is present in the crystal lattice (occupancy at 0.5); restraints were applied to regularize the C–C and C–N distances.

RESULTS AND DISCUSSION

Synthesis and Characterization. The hexafluorophosphate salts of seven ruthenium(II)-bis(phenanthrolinyl) complexes (**1**–**7**) and two ruthenium(II)-bis(bipyridyl) complexes (**8** and **9**) with a dpte ligand were synthesized by treating the appropriate *cis*-$Ru(diimine)_2Cl_2$ complex with excess dpte in 1:1 H_2O:ethanol solution (Schemes 1 and 2). The PF_6^- salts were isolated by anion metathesis to give yellow, orange, light

Scheme 1. Structures and Abbreviations for the Substituted 1,10-Phenanthroline and 2,2′-Bipyridine Ligands

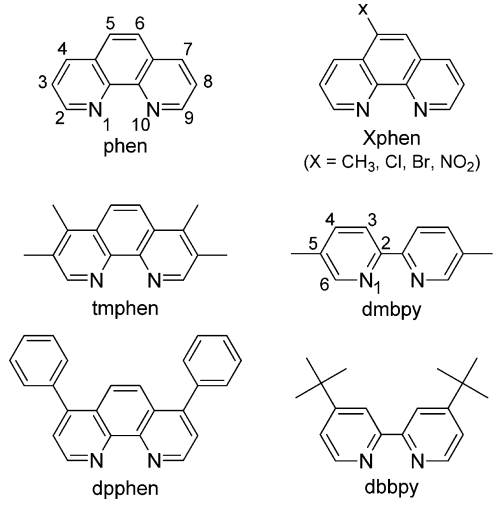

dx.doi.org/10.1021/ic4022454 | Inorg. Chem. 2014, 53, 294–307

Scheme 2. Synthetic Route and Numbering Scheme for $[Ru(diimine)_2(dpte)](PF_6)_2$

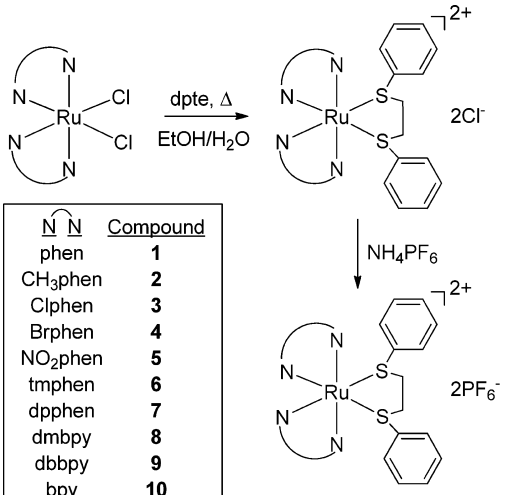

N N	Compound
phen	**1**
CH_3phen	**2**
Clphen	**3**
Brphen	**4**
NO_2phen	**5**
tmphen	**6**
dpphen	**7**
dmbpy	**8**
dbbpy	**9**
bpy	**10**

brown, or brown-black air-stable solids, which were purified by recrystallization or column chromatography. The compositions were confirmed by elemental analysis, ESI-TOF mass spectrometry and ^{1}H NMR spectroscopy.

The patterns of resonances in the ^{1}H NMR spectra are consistent with C_2 symmetry. The spectra show the expected influence of metal coordination on the diimine ligand chemical shifts,[77] namely, a large downfield shift of the *ortho*-proton resonances, a somewhat smaller influence on the *meta*-proton resonances, and a very small effect on the *para*-proton resonances with respect to free ligand resonances. Approximately half of the diimine ligand resonances occur in the 7.3–8.0 ppm range, whereas the remaining resonances are shifted further downfield (8–10 ppm), closer to those of the free ligand resonances. For each of the two sets of phenanthrolinyl *ortho*-proton resonances, there is a qualitative correlation with the electron-donor properties of the ligand substituents, characterized by a downfield shift along the series tmphen < CH_3phen < phen < Brphen, Clphen, dpphen < NO_2phen.

Interestingly, the dpte phenyl proton chemical shifts follow a characteristic order,[60,61] *ortho* (6.1–6.5 ppm) < *meta* (6.5–6.9 ppm) < *para* (6.6–7.2 ppm), but occur significantly upfield of those of the free ligand (7.3–7.4 ppm) and even further from those of square-planar platinum(II) complexes.[78] These observations are consistent with the presence of $\pi-\pi$ interactions between the phenyl rings and the diimine ligands (*vide infra*). For each complex, the methylene protons give rise to two apparent doublets (6–8 Hz) in the 3.0–3.3 and 3.8–4.0 ppm ranges, respectively. Similar patterns appear in the spectra of $Ru(bpy)_2(CH_3S(CH_2)_2SCH_3)^{2+}$ and $Ru(phen)_2(dpte)^{2+}$,[60,61] as well as $Ru(bpy)_2(tmen)^{2+}$ (tmen = *N*,*N*,*N*′,*N*′-tetramethylethylenediamine).[79] By analogy to earlier work,[60] we assign these resonances to a poorly resolved AA′XX′ pattern. Overall, the data are consistent with a single dpte conformation, but we do not rule out the possibility of rapidly interconverting conformers. For example, we anticipate that inversion about the S atoms of the dpte ligand is slow at room temperature, whereas flipping of the $-CH_2CH_2-$ dpte backbone is likely more rapid.[80–82]

Crystals of several of the salts (**2**, **5**, **7**, **9**) were readily grown by vapor diffusion of diethyl ether into ethanol–acetone or acetonitrile solutions. Interestingly, attempts to grow crystals of $[Ru(dmbpy)_2(dpte)](PF_6)_2$ (**8**) in room light repeatedly afforded orange crystals of $[Ru(dmbpy)_2(CH_3CN)_2](PF_6)_2$ (**8P**), in which the dpte ligand is replaced with two acetonitrile ligands. The overall conversion of **8** to **8P** can be described as

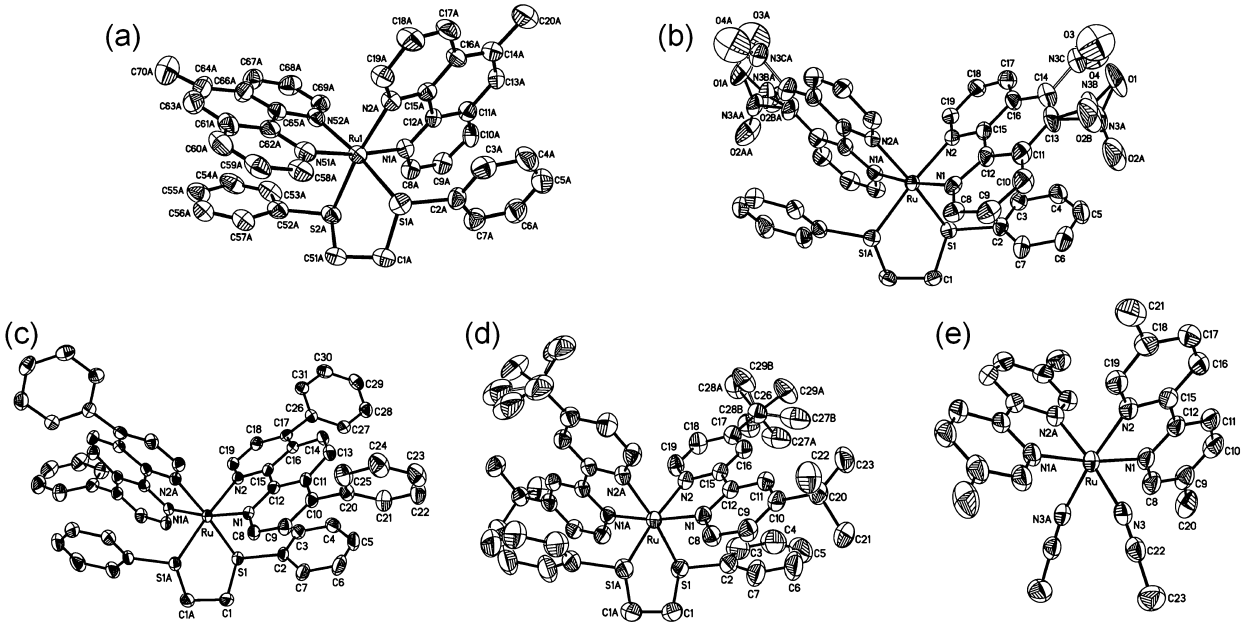

Figure 1. ORTEP diagrams of the cations of (a) $[Ru(CH_3phen)_2(dpte)](PF_6)_2 \cdot 0.5Et_2O$ (**2**·0.5Et_2O) (only 1 independent molecule shown), (b) $[Ru(NO_2phen)_2(dpte)](PF_6)_2 \cdot 4/3CH_3CN$ (**5**·4/3CH_3CN), (c) $[Ru(dpphen)_2(dpte)](PF_6)_2 \cdot 2CH_3CN$ (**7**·2CH_3CN), (d) $[Ru(dbbpy)_2(dpte)](PF_6)_2 \cdot CH_3CN$ (**9**·CH_3CN), and (e) $[Ru(5,5'\text{-dmbpy})_2(CH_3CN)_2](PF_6)_2$ (**8P**). H atoms are omitted for clarity. Displacement parameters at 30% probability level for **5**·4/3CH_3CN and 50% for all others.

dx.doi.org/10.1021/ic4022454 | *Inorg. Chem.* 2014, 53, 294–307

$$[Ru(dmbpy)_2(dpte)]^{2+} \xrightarrow[CH_3CN]{h\nu} [Ru(dmbpy)_2(CH_3CN)_2]^{2+} + dpte$$

This behavior is reminiscent of the photosubstitution chemistry of ruthenium(II) complexes with N-heterocyclic chelating ligands,[83−86] and the results are consistent with Collin's observation for the photolysis of $Ru(phen)_2(dpte)^{2+}$.[61]

X-ray Crystallography. The coordination geometries of the cations in **2**, **5**, **7**, **9**, and **8P** were confirmed by single-crystal X-ray crystallography (Figure 1; Table 1; and Table S1, Supporting Information). The metal−ligand bond lengths (Ru−N, 2.06−2.09 Å; Ru−S, 2.33−2.36 Å) and bond angles are normal and in good agreement with values reported for other ruthenium(II) diimine[87] and thioether complexes.[61,88] Overall, the geometries of the cations are similar to those of related compounds, such as $Ru(phen)_2(dpte)^{2+}$,[61] $Ru(phen)_2$-(2,2′-bipyrimidine)$^{2+}$,[89] and $Ru(bpy)_2(phen)^{2+}$.[90]

For each of the cations in **2**, **5**, **7**, and **9**, we can conceive of 12 isomers, resulting from configurational isomerism (Λ, Δ), as well as conformational isomerism due to the relative orientation of the dpte phenyl groups (syn, anti) and the conformation of the $-CH_2CH_2-$ dpte ligand backbone (λ, δ). To specify the stereochemical configuration at each S-donor atom, we use Cahn−Ingold−Prelog sequence rules ($-Ru^{2+}$ > −Ph > $-CH_2CH_2S$ > lone pair).[91] For each configurational isomer (Λ or Δ) with a given dpte ligand backbone conformation (λ or δ), there are three possible configurations for the pair of S atoms, *R,R*, *S,S*, and *R,S*. Interestingly, in these four crystal structures, as well as that of $[Ru(phen)_2(dpte)](PF_6)_2$,[61] the cation exclusively adopts the enantiomeric Δδ(*S,S*) and Λλ(*R,R*) configurations. Disregarding the diimine substituents, these isomers have crystallographically imposed C_2 symmetry in the structures of **5**, **7**, and **9** and approximate C_2 symmetry in the case of **2**. In crystals of $Pd(dpte)Cl_2$,[92] the dpte ligand adopts a similar conformation, namely, δ(*S,S*) and λ(*R,R*). By contrast, for six isostructural square-planar $Pt(dpte)(X)_2$ and Pt(dpte)(X)(Y) (X, Y = Cl, Br, I) complexes,[93] as well as for three complexes with fluorinated analogues of dpte,[94] only the δ(*R,R*) and λ(*S,S*) conformations are observed in the solid state, each having approximate C_2 symmetry. The δ(*S,S*) and λ(*R,R*) isomers favored by the ruthenium complexes are distinguished from δ(*R,R*) and λ(*S,S*) platinum complexes by the C(Ph)−S−CH_2−CH_2 torsion angles. The average of the mean angle is 162.5(9)° for the five ruthenium(II) structures (including the bpy derivative) and 77(3)° for eight platinum(II) complexes. Molecular models indicate that the preferred conformations for the ruthenium(II) bis-diimine complexes, Δδ(*S,S*) and Λλ(*R,R*), can be rationalized, at least in part, in terms of the reduced steric repulsion between the phenyl groups and α-H atoms of the diimine ligands, as compared to some of the other possible conformations. This results in a rather compact geometry, characterized by small dihedral angles (<24°; average mean angle for 5 structures: 18(3)°) and short contacts (<3.4 Å) between each phenyl group and the closest diimine ligand. Such π−π interactions are likely responsible for the upfield shift of the dpte resonances as compared to those of the free ligand and platinum(II) complexes.

In the cases of the complexes with phenanthrolinyl ligands substituted at the 5-position (**2** and **5**), there also are three possible geometric isomers of each enantiomer. Two have C_2 symmetry and are distinguished by the relative positions of the phenanthroline N-donor atoms at the 1-position (i.e., the N atom nearest the 5-position), which are either mutually *cis* or *trans*. A third isomer has C_1 symmetry and has the 1-position N atoms in a mutually *cis* arrangement. Assuming no chemical preference for one isomer over the others, a statistical distribution would correspond to a 2:1:1 ratio of the C_1:C_2(*trans*):C_2(*cis*) isomers. In crystals of **2**, the C_1 and C_2(*cis*) isomers are present in a 1:3 ratio, and there is no C_2(*trans*) isomer. For **5**, the exact distribution is not certain because of disorder. However, the refined relative occupancies of the NO_2 group bonded to C13 (67%) and C14 (33%) positions deviate from the expected 1:1 ratio (i.e., C13, 50%; C14, 50%). We can find no compelling reason for the presence of these nonstatistical distributions of geometric isomers in the reaction products, and therefore, it appears that the observed distributions are selected for in the crystallization process.

Electrochemistry. Cyclic voltammograms (CVs) of **1**−**10** exhibit waves characteristic of ruthenium diimine complexes,[74,95−97] including a nearly electrochemically and chemically reversible process in the 1.42−1.72 V vs Ag/AgCl range due to the Ru(III/II) couple (Table 2). The anodic−cathodic peak separations ($\Delta E_p = E_{pa} - E_{pc}$) of the latter vary between 59 and 70 mV and are nearly scan-rate independent. The ratios of the cathodic to anodic peak currents (i_{pc}/i_{pa}) were typically 0.9−1.0. Each complex also exhibits two ligand-based reduction waves[74,98] with $E^{\circ\prime}(L^{0/-})$ and $E^{\circ\prime}(L^{-/2-})$ values falling in the −1.17 to −1.72 and the −1.42 to −1.89 V ranges, respectively. Values of ΔE_p for the first reduction are scan-rate independent and vary between 60 and 90 mV, which is not atypical.[96] In the case of **5**, the first reduction process (−1.17 V) is quasi-reversible; on the basis of the redox chemistry of the free ligand and other nitroaromatics,[63,99,100] we cannot exclude the possibility that this process involves reduction of the nitro group. In all cases, the second reduction process is chemically irreversible. The CVs of several complexes show a third irreversible wave in the −1.7 to −1.9 V range, which is attributable to chemical product(s) formed at more positive potentials.

Table 2. Electrochemical Data ($E^{\circ\prime}$) for $Ru(L)_2(dpte)^{2+}$ Complexes (L = Diimine) in Acetonitrile

	$E^{\circ\prime}$ (V vs Ag/AgCl (3.0 M NaCl))			
compound	$Ru^{3+/2+}$	$L^{0/-}$	$L^{-/2-}$	3rd reduction
1	1.60	−1.21	−1.42[a]	
2	1.57	−1.34	−1.54[a]	
3	1.65	−1.20	−1.55[a]	−1.74[a]
4	1.64	−1.19	−1.53[a]	−1.77[a]
5	1.72	−1.17[b]	−1.53[a]	
6	1.42	−1.72	−1.89[a]	
7	1.53	−1.46	−1.64[a]	
8	1.50	−1.46	−1.66[a]	−1.90[a]
9	1.47	−1.59	−1.85[b]	
10[c]	1.50			

[a]Irreversible, reported as the cathodic peak potential (E_{pc}). [b]Quasi-reversible. [c]Reference 60.

Overall, the redox properties of the $Ru(diimine)_2(dpte)^{2+}$ series can be rationalized in terms of the relative donor properties of the ligands. For example, comparison with other $Ru^{II}(diimine)_2(LL)^{n+}$ complexes reveals that $E^{\circ\prime}(Ru^{3+/2+})$ lies intermediate between values for complexes where LL is a

dx.doi.org/10.1021/ic4022454 | Inorg. Chem. 2014, 53, 294−307

diimine ligand (e.g., $Ru^{II}(phen)_3^{n+}$, 1.31 V vs Ag/AgCl)[101] and complexes where LL is a phosphine chelate (e.g., $Ru(bpy)_2(dppp)^{2+}$, 1.79 V; dppp = 1,3-bis(diphenylphosphino)propane),[74] in keeping with the expected poor σ-donor properties and high π-acidity of thioether ligands.[102,103] Within the series of phenanthrolinyl ligands substituted at the 5-position, $E^{o\prime}(Ru^{3+/2+})$ increases as the substituent becomes more electron-withdrawing along the series: CH_3 < H < Br, Cl < NO_2 (*vide infra*). $E^{o\prime}(L^{0/-})$ varies over a wider range than $E^{o\prime}(Ru^{3+/2+})$, but the results are qualitatively similar, with $E^{o\prime}(L^{0/-})$ shifting to more positive values as the diimine ligand subsitutents become more electron-withdrawing. Taken together, the data are consistent with the view that the diimine substituents influence the energies of the mainly metal-based HOMO and mainly diimine ligand-based LUMO but have a greater effect on the LUMO.

Electronic Spectroscopy. In acetonitrile solution, each complex exhibits an intense ((6−9) × 10^3 M^{-1} cm^{-1}) MLCT [dπ(Ru) → π_1*(diimine)] absorption band maximizing in the 375−410 nm range (Figure 2, Table 3). The band occurs at

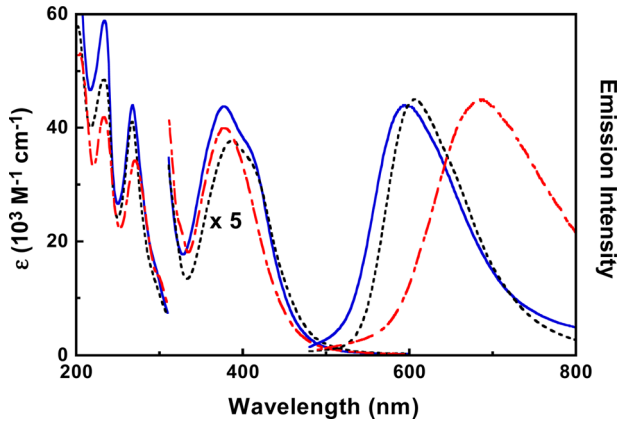

Figure 2. Absorption and emission spectra of **2** (——), **3** (- - -), and **6** (- —— -) in room-temperature acetonitrile solution.

Table 3. Room-Temperature MLCT Absorption Maxima (λ_{abs}), Emission Maxima (λ_{em}), and Excited-State Lifetimes (τ) for 1−10 in Acetonitrile

compound[a]	λ_{abs} (nm)	λ_{em} (nm)	τ (ns)[b]
1	378	597	278
2	377	594	245
3	389	606	351
4	387	608	335
5	408	635	742
6	375	687	140
7	398	610	639
8	396	673	254
9	390	625	571
10[a]	404		

[a]Reference 60. [b]Degassed solution.

significantly shorter wavelengths than found for many $[Ru(diimine)_2(LL)]^{2+}$ complexes[74] and lies near maxima for arylphosphines (e.g., $[Ru(bpy)_2(dppm)]^{2+}$, 384 nm, dppm = bis(diphenylphosphinomethane).[60] This is a consequence of the comparatively high π-acidity of the thioether donor ligand, which stabilizes the dπ(Ru) levels and blue-shifts the MLCT band. In keeping with the expected influence of the diimine ligand substituents on the relative energies of the dπ(Ru) and π*(diimine) levels,[15,25] the MLCT band maxima for **1**−**7** shift from to 375 to 408 nm along the tmphen < CH_3phen, phen < Brphen, Clphen < dpphen < NO_2phen series, varying over a 2150 cm^{-1} range. In the spectra of several complexes (**1**, **2**, **3**, **4**, and **7**), the MLCT band appears with a long-wavelength shoulder shifted ~2000 cm^{-1} from the maximum; this is tentatively attributed to a formally spin-forbidden MLCT transition.

In the UV region (Figure 2; Table S2, Supporting Information), the spectra of the phenanthrolinyl complexes show two strong absorption bands near 230 and 270 nm ((3−6) × 10^4 M^{-1} cm^{-1}). In the case of the longer wavelength band, a similar feature appears in the 77 K absorption spectra of $Ru(phen)_3^{2+}$ (~275 nm), $Rh(phen)_3^{2+}$ (~265 nm),[104] and $Pt(phen)_2^{2+}$ (267 nm)[105] Accordingly, the band is assigned to a phenanthrolinyl ligand-centered transition. The bipyridyl complexes also exhibit two intense absorption features near 240 and 290 nm ((4−5) × 10^5 M^{-1} cm^{-1}) with a shoulder near 260 nm. From comparison with the spectra of the protonated ligands,[106] the two bands are assigned to the bipyridyl ligand-centered (LC) π → π_1* and π → π_2* transitions, respectively. Similar transitions are observed in the spectra of platinum(II) and iridium(III) complexes.[104,107] In support of the π → π_1* assignments, this band is shifted to the red by ~1000 cm^{-1} in the spectrum of **8**, as compared to **9** and **10**. This behavior is consistent with the influence of hyperconjugation on π → π* transitions polarized along the axis defined by the 5- and 5′-carbon atoms, as we have previously described for platinum(II) bipyridyl complexes.[108] It also may be noted that the MLCT[dπ(Ru) → S] band for $Ru(dpte)_2Cl_2$ occurs at 313 nm (1.5 × 10^3 M^{-1} cm^{-1}).[64] However, the metal-based redox potentials of **1**−**10** (*vide supra*) are ~1 V higher than that of $Ru(dpte)_2Cl_2$, and therefore, the corresponding transition in the spectra of **1**−**10** likely occurs at significantly shorter wavelengths where it is obscured by ligand-centered transitions. In the case of **5**, an additional band occurs as a shoulder near 330 nm (7.8 × 10^3 M^{-1} cm^{-1}). A similar feature appears in the spectrum of $Ru(NO_2phen)_3^{2+}$ and has been assigned as an n → π* transition of the NO_2 group.[109]

Emission Spectroscopy. Though ruthenium(II) bis-diimine complexes with π-acidic phosphine ligands are typically nonemissive in room-temperature fluid solution,[110−112] the complexes reported here give rise to reasonably intense emissions. The bands are broad (fwhm, ~4000 cm^{-1}) and structureless with slight asymmetry, which manifests as a tailing to longer wavelengths (Figure 2). The maxima vary over a ~2300 cm^{-1} range from 594 to 687 nm (Table 3). In most cases, the emissions are assigned as originating from a lowest MLCT[dπ(Ru) → π_1*(diimine)] state. The lifetimes fall in the 140−740 ns range, which is consistent with spin-forbidden character of the excited state. Overall and as observed for the MLCT absorption band, the results are qualitatively consistent with changes in the diimine ligand substituents, which are expected to influence the unoccupied π*(diimine) level, as well as the occupied dπ(Ru) levels to a lesser extent.[15,25] In support of this assignment, the emission maxima for **1**−**5** shift slightly to longer wavelengths along the CH_3phen ≈ phen < Clphen ≈ Brphen < NO_2phen series. The trend is similar to that observed for the MLCT absorption band and is consistent with the increasing electron-acceptor properties of the substituent X (CH_3 < H < Cl, Br < NO_2) at the 5-position of the phenanthrolinyl ligand. Interestingly, for **1**−**5**, the emission

dx.doi.org/10.1021/ic4022454 | Inorg. Chem. 2014, 53, 294−307

maxima only span a 1000 cm^{-1} range, which is roughly half that of the ^{1}MLCT absorption band. This behavior is reminiscent of that noted for $Os(bpy)_2(LL)^{2+}$ and $Os(phen)_2(LL)^{2+}$ complexes with nonchromophoric LL ligands; in those systems, the MLCT emission energies span about half the range as the corresponding absorption energies.[23] The effect has been attributed to increasing contribution of nuclear displacement to the Franck−Condon energies with increasing energy gap. The rather long lifetime for the NO_2phen complex (**5**, 742 ns) is somewhat surprising because complexes with this ligand are frequently nonemissive at room temperature due to a low-lying, intraligand n → π^* excited state.[77,113] It is noteworthy that previous studies suggest a switching in the orbital character of the LUMO of W(0) and Pt(II) phenanthrolinyl complexes upon replacing phen with NO_2phen.[114−116] Also, the emission maximum of **6** occurs at longer wavelengths and is shorter-lived (λ_{max}, 687 nm; 140 ns) than that found for the other complexes, which may signify different orbital parentage of the emitting state.

Correlation of $E^{\circ\prime}(Ru^{3+/2+})$ with Hammett Parameters. To assess the influence of phenanthrolinyl ligand substituents on the $Ru^{3+/2+}$ couple, we have explored empirical linear correlations of the metal-based redox potential (vs NHE) of **1**−**7** with a summative Hammett parameter, σ_T

$$E^{\circ\prime}(Ru^{3+/2+}) = \alpha\sigma_T + \beta \quad (1)$$

where α and β are the fitted slope and intercept, respectively. The 27 parametrizations are distinguished by $\sigma_T[\sigma(3,8);\sigma(4,7);\sigma(5,6)]$, which is the sum of substituent parameters (σ_m, σ_p, and/or σ_p^+) used to describe substituents at the 3,8-, 4,7-, and 5,6-positions of each diimine ligand of a complex:

$$\sigma_T[\sigma(3,8);\ \sigma(4,7);\ \sigma(5,6)] = \sum_i \sum_j \sigma_{i,j} \quad (2)$$

The substituent constant for phenanthrolinyl ligand i at position j is given by $\sigma_{i,j}$, where j ranges from position 2 to 8.[117] The Pearson product-moment correlation coefficient (R) was used as a measure of the linear correlation between $E^{\circ\prime}(Ru^{3+/2+})$ and σ_T. To find the strongest correlation, we considered parametrizations with σ_p and/or σ_p^+ (as well as σ_m) for $\sigma(3,8)$ and $\sigma(5,6)$, which can be rationalized if there are significant mesomeric effects at these positions in the phenanthrolinyl ligands. The strongest correlations occur for eight of the nine cases with σ_T having $\sigma(4,7) = \sigma^+$ (R, 0.973−0.995). The strongest of these involves $\sigma_T[\sigma_m;\sigma_p^+;\sigma_m]$ (R, 0.995; Figure 3; Table 4). Correlations with σ_p^+ have been noted for $Ru(4,4'\text{-}(X)_2\text{-}bpy)_3^{2+}$ complexes with X substituents at the 4- and 4′-positions of bipyridyl ligands.[38] Interestingly, the slope (=0.4) of a plot of $E^{\circ\prime}(Ru^{3+/2+})$ for the five $Ru(Xphen)_3^{2+}$ complexes with Xphen ligands (i.e., **1**−**5**) vs $E^{\circ\prime}(Ru^{3+/2+})$ of their $Ru(4,4'\text{-}(X)_2\text{-}bpy)_3^{2+}$ counterparts with X substituents at the 4- and 4′-positions of bipyridyl ligands was not significantly less than 0.5 (X = H, Cl, Br, Me, Ph). Thus, it would appear that, within this limited data set, placement of a substituent at the 5-position of 1,10-phenanthroline has roughly half the effect of introducing substituents at *both* the 4- and 4′-positions of 2,2′-bipyridine.[117]

For comparison and to explore the generality of these parametrizations for ruthenium complexes with phenanthrolinyl ligands (as well as bipyridyl ligands), we extended this analysis to previously reported redox potentials for tris-diimine complexes. The three data sets explored here are given in Tables S7−S9 (Supporting Information): (**A**) 13 tris-phenanthrolinyl complexes (27 measurements), (**B**) 57 tris-bipyridyl complexes (135 measurements), and (**C**) 27 mixed-ligand complexes (32 measurements) where each contains at least one bipyridyl and one phenanthrolinyl ligand. In instances of replicate measurements (i.e., reports on the same complex in different publications), average values of $E^{\circ\prime}(Ru^{3+/2+})$ were used. The summative Hammett parameter for data set **B** is given by

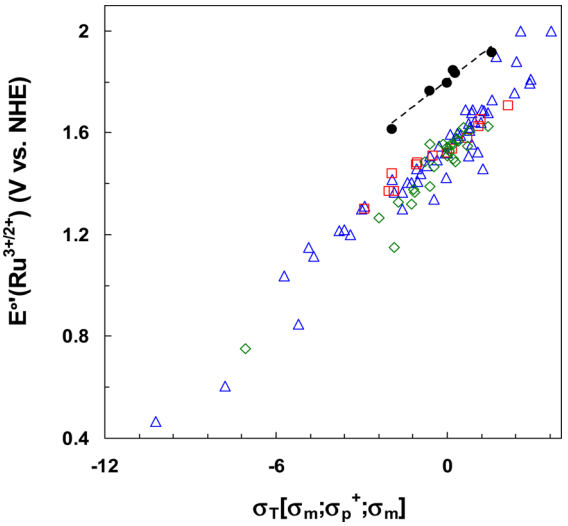

Figure 3. Plot of $E^{\circ\prime}(Ru^{3+/2+})$ for **1**−**7** (black circle), 57 tris-bipyridyl complexes (data set **A**, blue triangle), 13 tris-phenanthrolinyl complexes (data set **B**, red square), and 33 mixed-ligand complexes (data set **C**, green diamond) vs $\sigma_T[\sigma_m;\sigma_p^+;\sigma_m]$. Dashed line shows best fit for **1**−**7**: $E^{\circ\prime}(Ru^{3+/2+}) = 0.0862\ \sigma_T + 1.785$ (V vs NHE).

$$\sigma_T[\sigma(3,3');\sigma(4,4')] = \sum_i \sum_j \sigma_{i,j} \quad (3)$$

For the mixed bipyridyl/phenanthrolinyl ligand data set **C**, we required $\sigma(3,3') = \sigma(3,8)$ and $\sigma(4,4') = \sigma(4,7)$.

Each data set shows strong correlations with specific σ_T parametrizations; the strongest are shown in Table 4. The most striking finding is that use of σ_p^+ (vs σ_m or σ_p) for $\sigma(4,4')$ and $\sigma(4,7)$ consistently resulted in stronger correlations, just as we found for **1**−**7**. For example, in the case of the 57 tris-bipyridyl complexes making up data set **B**, the correlation coefficient for the best parametrization ($\sigma_T[\sigma_p;\sigma_p^+]$, $R = 0.976$) is significantly greater than that for parametrizations having $\sigma(4,4') \neq \sigma_p^+$ ($R < 0.95$). The superiority of σ^+ in describing 4,4′-position substituent effects in a subset of 10 tris-bipyridyl complexes (i.e., $Ru(4,4'\text{-}(X)_2\text{-}bpy)_3^{2+}$) previously was rationalized in terms of the emerging positive charge during oxidation of the Ru(II) center.[38] These findings can be understood in terms of dπ/π^* overlap since this allows for contribution from resonance structures that delocalize the positive charge on the metal to the 4- and 4′-positions of bipyridyl ligands, as well as the 4- and 7-positions of phenanthrolinyl ligands. The correlation coefficients are less strongly dependent on the choice of $\sigma(3,3')$ for bipyridyl ligands or $\sigma(3,8)$ and $\sigma(5,6)$ for phenanthrolinyl ligands. Therefore, the statistical justification for selecting specific parametrizations at these positions is somewhat weaker.

Taking $\sigma(3,3') = \sigma(3,8)$ and $\sigma(4,4') = \sigma(4,7)$, plots of $E^{\circ\prime}(Ru^{3+/2+})$ vs σ_T for the best parametrizations (i.e., $\sigma(4,4') = \sigma(4,7) = \sigma_p^+$) show that data from sets **A**, **B**, and **C** are clustered

dx.doi.org/10.1021/ic4022454 | *Inorg. Chem.* 2014, 53, 294−307

Table 4. Regression Results for $E^{\circ\prime}(Ru^{3+/2+})$ on Best Parameterizations of σ_T

data set	σ_T	α (V vs NHE)	β (V vs NHE)	R	N
compounds **1**−**7**	$\sigma_T[\sigma_m;\sigma_p^+;\sigma_m]$	0.086 ± 0.010	1.785 ± 0.010	0.995	7
A (tris-phenanthrolinyl)	$\sigma_T[\sigma_m;\sigma_p^+;\sigma_m]$	0.078 ± 0.009	1.541 ± 0.014	0.984	13
B (tris-bipyridyl)	$\sigma_T[\sigma_m;\sigma_p^+]$	0.106 ± 0.006	1.547 ± 0.017	0.976	57
C (mixed diimine)	$\sigma_T[\sigma_m;\sigma_p^+;\sigma_m]$	0.111 ± 0.014	1.516 ± 0.022	0.957	27

Table 5. Electrochemical Parameters (E_L), Number of Compounds, and Number of Measurements for dpte and Diimine Ligands Appearing in More than One Compound

ligand[a,b]	E_L	ligand[a,b]	E_L
dpte (10, 10)	0.380 ± 0.016	CH_3phen (4, 4)	0.253 ± 0.012
5,5′-dtfmbpy (3, 3)	0.338 ± 0.012	dpphen (3, 4)	0.243 ± 0.009
4,4′-dtfmbpy (3, 3)	0.337 ± 0.012	4,4′-dphbpy (3, 7)	0.243 ± 0.008
4,4′-dcmbpy (3, 3)	0.303 ± 0.012	5,6-dmphen (2, 2)	0.241 ± 0.013
4,4′-$(COOEt)_2$-bpy (7, 11)	0.302 ± 0.007	4,4′-dmbpy (16, 34)	0.228 ± 0.004
4-NO_2-bpy (2, 4)	0.293 ± 0.009	dbbpy (4, 6)	0.228 ± 0.008
NO_2phen (5, 7)	0.284 ± 0.008	4-Me-4′-vinyl-bpy (7, 7)	0.224 ± 0.012
4-COOH-4′-Me-bpy (2, 2)	0.279 ± 0.033	4,7-dmphen (3, 3)	0.222 ± 0.012
5-Br-bpy (2, 2)	0.274 ± 0.013	tmbpy (2, 2)	0.216 ± 0.014
Brphen (2, 2)	0.273 ± 0.013	3,4,7,8-tmphen (3, 3)	0.213 ± 0.011
Clphen (4, 5)	0.270 ± 0.009	4,4′-$(MeO)_2$-bpy (2, 4)	0.184 ± 0.009
4,4′-$(COOH)_2$-bpy (2, 5)	0.269 ± 0.014	4,7-$(HO)_2$-phen (2, 2)	0.132 ± 0.021
phphen (3, 3)	0.256 ± 0.010	4,4′-$(NEt_2)_2$-bpy (3, 6)	0.099 ± 0.007
phen (9, 21)	0.254 ± 0.004	4,4′-$(NH_2)_2$-bpy (2, 3)	0.098 ± 0.010
bpy (44, 98)	0.253 ± 0.002	4,4′-$(NMe_2)_2$-bpy (3, 4)	0.080 ± 0.010

[a](No. of compounds containing ligand, no. of measurements). [b]5,5′-dtfmbpy = 5,5′-ditrifluoromethyl-2,2′-bipyridine; 4,4′-dtfmbpy = 4,4′-ditrifluoromethyl-2,2′-bipyridine; 4,4′-dcmbpy = 4,4′-dicarbomethoxy-2,2′-bipyridine; 4,4′-$(COOEt)_2$-bpy = 4,4′-dicarboethoxy-2,2′-bipyridine; 4-NO_2-bpy = 4-nitro-2,2′-bipyridine; 4-COOH-4′-Me-bpy = 4-carboxyl-4′-methyl-2,2′-bipyridine; NO_2phen = 5-nitro-1,10-phenanthroline; 5-Br-bpy = 5-bromo-2,2′-bipyridine; Brphen = 5-bromo-1,10-phenanthroline; Clphen = 5-chloro-1,10-phenanthroline; 4,4′-$(COOH)_2$-bpy = 4,4′-dicarboxyl-2,2′-bipyridine; phphen = 5-phenyl-1,10-phenanthroline; CH_3phen = 5-methyl-1,10-phenanthroline; dpphen = 4,7-diphenyl-1,10-phenanthroline; 4,4′-dphbpy = 4,4′-diphenyl-2,2′-bipyridine; 5,6-dmphen = 5,6-dimethyl-1,10-phenanthroline; 4,4′-dmbpy = 4,4′-dimethyl-2,2′-bipyridine; dbbpy = 4,4′-di-*tert*-butyl-2,2′-bipyridine; 4-Me-4′-vinyl-bpy = 4-methyl-4′-vinyl-2,2′-bipyridine; 4,7-dmphen = 4,7-dimethyl-1,10-phenanthroline; tmbpy = 3,3′,4,4′-tetramethyl-2,2′-bipyridine; 3,4,7,8-tmphen = 3,4,7,8-tetramethyl-1,10-phenanthroline; 4,4′-$(MeO)_2$-bpy = 4,4′-dimethoxy-2,2′-bipyridine; 4,7-$(HO)_2$-phen = 4,7-dihydroxy-1,10-phenanthroline; 4,4′-$(NEt_2)_2$-bpy = 4,4′-diethylamino-2,2′-bipyridine; 4,4′-$(NH_2)_2$-bpy = 4,4′-diamino-2,2′-bipyridine; 4,4′-$(NMe_2)_2$-bpy = 4,4′-dimethylamino-2,2′-bipyridine.

together (e.g., Figure 3). Likewise, regression parameter estimates for data sets **A**, **B**, and **C** tend to be similar for a given σ_T parametrization (Table 4). Similar intercepts, corresponding to $\sigma_T = 0$, are not surprising because values of $E^{\circ\prime}(Ru^{3+/2+})$ for $Ru(bpy)_3^{2+}$, $Ru(phen)_3^{2+}$, $Ru(bpy)_2(phen)^{2+}$, and $Ru(bpy)(phen)_2^{2+}$ are almost identical. Thus, one could be tempted to treat **A**, **B**, and **C** as if they arose from the same population and follow the same regression equation. Aside from chemical concerns, such as the fact that the donor properties of phen clearly are not identical to those of bpy, the hypothesis that the three data sets obey the same regression equation is not statistically significant. Moreover, the strongest regression relationship for the tris-bipyridyl data set **B** involves $\sigma_T[\sigma_p;\sigma_p^+]$, whereas those for **A** and **C** involve a different parametrization, namely, $\sigma_T[\sigma_m;\sigma_p^+;\sigma_m]$. Therefore, we recommend treating such data separately, and we favor $\sigma_T[\sigma_p;\sigma_p^+]$ for tris-bipyridyl complexes and $\sigma_T[\sigma_m;\sigma_p^+;\sigma_m]$ for tris-phenanthrolinyl complexes.

Altogether, the results for **1**−**7** and each of the tris-diimine data sets suggest that eq 1 has practical utility in the prediction of $E^{\circ\prime}(Ru^{3+/2+})$. As shown in Figure 3, a plot of $E^{\circ\prime}(Ru^{3+/2+})$ vs $\sigma_T[\sigma_m;\sigma_p^+;\sigma_m]$ for **1**−**7** is shifted vertically by ∼0.24 V from that for tris-phenanthrolinyl complexes (data set **A**). This is consistent with the weaker donor properties of dpte as compared to those of phen. For example, σ_T is 0 for $Ru(phen)_2(dpte)^{2+}$ (1.80 V vs NHE) and $Ru(phen)_3^{2+}$ (1.52 V vs NHE), but the dpte complex has a significantly higher value of $E^{\circ\prime}(Ru^{3+/2+})$. On the other hand, the slopes (α in Table 4) of plots of $E^{\circ\prime}(Ru^{3+/2+})$ vs $\sigma_T[\sigma_m;\sigma_p^+;\sigma_m]$ for **1**−**7** and data set **A** are statistically identical. This agreement is further evidence of the predictive relationship between $E^{\circ\prime}(Ru^{3+/2+})$ and the σ_m substituent constant for the 5- and 6-positions. Furthermore, it is apparent that, despite being further from the metal center, substituents at these positions exert influence on $E^{\circ\prime}(Ru^{3+/2+})$ that is comparable to that of substituents at the 3- and 8-positions.

E_L Parameters. Lever has employed the ligand additivity concept[46] to assign a ligand electrochemical parameter, E_L, to more than 200 ligands of ruthenium complexes, whereby $E(Ru^{3+/2+})$ vs NHE for a given complex can be estimated from the sum of the E_L parameters ($\sum E_L$) of the ligands bonded to the complex. Surprisingly, E_L values have been reported for only a few substituted phenanthrolinyl ligands,[44,45] and therefore, we were interested in extracting estimates from the data assembled here. We considered 199 measurements of $E(Ru^{3+/2+})$ for 58 tris-bipyridyl complexes, 13 tris-phenanthrolinyl complexes, and 27 $Ru(X)_2(Y)^{2+}$ and $Ru(X)(Y)_2^{2+}$ complexes where X is a bipyridyl ligand and Y is a phenanthrolinyl ligand (Table S3, Supporting Information). We chose to include replicate measurements rather than use averages, because this approach served to retain some information about the underlying variances. Addition of nine

dx.doi.org/10.1021/ic4022454 | Inorg. Chem. 2014, 53, 294−307

Table 6. Regression Results for E_L on Best Parameterizations of σ_T

ligand type	σ_T	f	E_L(LH)	R	N
phenanthrolines	$\sigma_T[\sigma_p;\sigma_p^+;\sigma_m]$	0.060 ± 0.010	0.258 ± 0.006	0.943	20
	$\sigma_T[\sigma_m;\sigma_p^+;\sigma_m]$	0.056 ± 0.009	0.258 ± 0.006	0.943	20
bipyridines	$\sigma_T[\sigma_p;\sigma_p^+]$	0.048 ± 0.006	0.256 ± 0.007	0.951	35
	$\sigma_T[\sigma_m;\sigma_p]$	0.084 ± 0.011	0.234 ± 0.008	0.941	35
4-R- and 4,4′-R_2-bipyridines	$\sigma_T[\sigma_p^+]$	0.048 ± 0.006	0.258 ± 0.008	0.963	26
	$\sigma_T[\sigma_p]$	0.084 ± 0.011	0.234 ± 0.008	0.957	26

measurements for dpte complexes **1**−**9**, as well as an earlier report for $Ru(bpy)_2(dpte)^{2+}$ (**10**)[60] (Table S4, Supporting Information), yielded a data set of 209 measurements on 109 complexes. Multivariate linear regression (R^2, 0.999) produced estimates of E_L for 56 diimine ligands, as well as dpte (Figure S1, Supporting Information). For the 209 measurements, the correlation coefficient (R) between $E(Ru^{3+/2+})$ and $\sum E_L$ is 0.987. Large deviation from this relationship for one measurement[37] of $Ru(4,4'\text{-}(Et_2N)_2\text{-bpy})_3^{2+}$ calls into question the reliability of the reported $E(Ru^{3+/2+})$ value (Figure S1). E_L values for ligands appearing in two or more complexes are shown in Table 5. Other values are in Table S10 (Supporting Information). For previously parametrized ligands,[44,45] most values of E_L are within ≤0.01 V of earlier reports.

It also is of practical interest to estimate E_L from Hammett substituent parameters. By extension of earlier work,[39] E_L parameters for diimine ligands can be related to σ_T according to

$$E_L = f\sigma_T + E_L(LH) \quad (4)$$

where f is the slope and E_L(LH) is the estimated E_L for the unsubstituted diimine ligand. Regression data for bipyridyl and phenanthrolinyl ligands are summarized in Table 6. For 20 phenanthrolinyl ligands, correlations with $\sigma_T[\sigma_p;\sigma_p^+;\sigma_m]$ and $\sigma_T[\sigma_m;\sigma_p^+;\sigma_m]$ are the strongest and almost equally good,[118] but there is a clear preference for $\sigma(4,7) = \sigma_p^+$. For 35 bipyridyl ligands, the best correlation is with $\sigma_T[\sigma_p;\sigma_p^+]$, but it is not significantly higher than that with $\sigma_T[\sigma_m;\sigma_p]$, which is second best. The correlation is only slightly stronger for bpy and the 25 bipyridyl ligands having substitutents at only the 4- or 4,4′-positions (Table 6). Therefore, in relating E_L to Hammett parameters, we favor the use of $\sigma(4,7) = \sigma_p^+$ and $\sigma(5,6) = \sigma_m$ in the case of phenanthrolinyl ligands, and either $\sigma_T[\sigma_p;\sigma_p^+;\sigma_m]$ or $\sigma_T[\sigma_m;\sigma_p^+;\sigma_m]$ works well. Surprisingly, the choice of $\sigma(4,4')$ is less obvious in the case of bipyridyl ligands, and we recommend either $\sigma_T[\sigma_p;\sigma_p^+]$ or $\sigma_T[\sigma_m;\sigma_p]$. Taken together, the accumulated results indicate that eqs 1 and 4, along with the best parametrizations in Tables 4 and 6, allow for interconversion between estimates of E_L, σ_T, and $E(Ru^{3+/2+})$. We suggest that deviations from these relationships are an indication of unusual or suspect data.

Other Correlations. We were interested in delineating other correlations between redox and spectroscopic parameters with emphasis on complexes **1**−**5** with Xphen ligands. For example, a plot of the first diimine ligand reduction potential, $E^{o\prime}(L^{0/-})$, versus $E^{o\prime}(Ru^{3+/2+})$ for **1**−**9** gives a slope of 2.0 (R, 0.95; Figure S2, Supporting Information), indicating that the ligand-based reduction potential is approximately twice as sensitive to changes in the ligand as the metal-centered potential *for this particular series*. For **1**−**5** alone, the slope is 0.9 (R, 0.79). In either case, the slope is steeper than that found for 33 $[Ru(bpy)_2XY]^{n+}$ complexes (0.22), where X and Y are nondiimine ligands.[11] This is consistent with the reduction of the latter complexes being bpy-based and, therefore, comparatively less sensitive to variations in the ancillary XY ligands than the metal-based oxidation. Conversely, the ligand-based reduction of **1**−**9** is *more* sensitive to variations in diimine ligand substituents than is the metal-based oxidation. Related arguments account for rather shallow slopes in two series of $Ru(L)_n(bpy)_{3-n}^{2+}$ (n = 1, 2, 3) complexes in which the reduction is L-based (L = 2,2′-bipyrimidine, slope = 0.4; L = 2,2′-bipyrazine, slope = 0.5).[96] We find that the approximately linear $E^{o\prime}(L^{0/-})$ versus $E^{o\prime}(Ru^{3+/2+})$ relationship holds for several sets of ruthenium(II) complexes with substituted bipyridyl ligands (L) (Figure S3, Supporting Information): 5 $Ru(tpm)(py)(L)^{2+}$ complexes in acetonitrile (tpm = tris(1-pyrazolyl)methane; slope = 1.7; R, 0.97),[15] 6 $Ru(L)_3^{2+}$ complexes in DMF (slope = 1.6; R, 0.96),[29] and 11 $Ru(L)_3^{2+}$ complexes in acetonitrile (slope = 1.1, R, 0.98).

Earlier studies[5,44] anticipated the existence of correlations between redox potentials across different metal ions sharing common ligand sets. To assess this possibility for the Xphen ligand series, we identified three sets of homoleptic $M(Xphen)_m^{n+}$ complexes where, for each metal (M = Fe, Ni, Cu), there are four or all five of the Xphen ligands in **1**−**5**.[119−121] For a given metal, the plot of $E^{o\prime}(Ru^{3+/2+})$ versus the metal-based redox potential of $M(L)_m^{n+}$ is approximately linear (Figure S4, Supporting Information): $Fe(Xphen)_3^{3+/2+}$ (n = 5, slope = 0.6; R, 0.99), $Ni(Xphen)_3^{3+/2+}$ (n = 4; slope = 0.7; R, 0.99), and $Cu(Xphen)_2^{2+/+}$ (n = 4; slope = 1.1; R, 1.00). It is noteworthy that, in each case, the slope is approximately equal to the ratio of the number of Xphen ligands in the two sets of complexes (i.e., $2/m$).

One of the most well-known relationships between spectroscopic and redox parameters of ruthenium(II) complexes with bipyridyl ligands is the correlation of the MLCT absorption (E_{abs}) and emission (E_{em}) energies with ΔE, which is $E^{o\prime}(Ru^{3+/2+}) - E^{o\prime}(L^{0/-})$,[5−22] we use the room-temperature absorption and emission maxima as estimates of E_{abs} and E_{em}, respectively. For **1**−**10**, this relationship decidedly does *not* hold, even when **5** (NO_2phen) and **6** (tmphen) are excluded. It would appear that the underlying assumptions of the constancy of the reorganization energy, configuration interaction, and the orbital character of the excited states do not hold across the series. For the **1**−**5** subset, the correlation also is poor, but ΔE only varies by 0.1 V, so no definitive conclusions can be reached.

On the other hand, E_{abs} and E_{em} for **1**−**5** are strongly correlated, such that a plot of E_{em} versus E_{abs} has a slope (=0.52; R, 0.99; Figure S5, Supporting Information) that is significantly less than 1 and consistent with greater variation in E_{abs} (*vide supra*). Moreover, E_{abs} and E_{em} show an approximate linear relationship with $E^{o\prime}(Ru^{3+/2+})$ (E_{abs}, -14.0×10^3 cm^{-1}/V, R = −0.98; E_{em}, -7.3×10^3 cm^{-1}/V, R = −0.97; Figure S6, Supporting Information), whereas correlations with the ligand-based reduction potential $E^{o\prime}(L^{0/-})$ are poor ($|R| < 0.67$). The existence of the former relationships reflects a degree of self-

dx.doi.org/10.1021/ic4022454 | Inorg. Chem. 2014, 53, 294−307

consistency among the E_{abs}, E_{em}, and $E^{\circ\prime}(Ru^{3+/2+})$ values for **1**−**5** and is in keeping with the notion that the absorption and emission bands both arise from MLCT transitions. Moreover, E_{abs} and E_{em} show strong negative linear correlations with Hammett parameters σ_m, σ_p, and σ_p^+ for the X group of the Xphen ligand. In contrast to the aforementioned results showing that $E^{\circ\prime}(Ru^{3+/2+})$ is most strongly correlated with σ_m, E_{abs} and E_{em} are more strongly correlated with σ_p ($R \leq -0.99$; Figure 4) than either σ_p^+ (E_{abs}, $R = -0.96$; E_{em}, $R = -0.98$) or σ_m (E_{abs}, $R = -0.95$; E_{em}, $R = -0.93$).

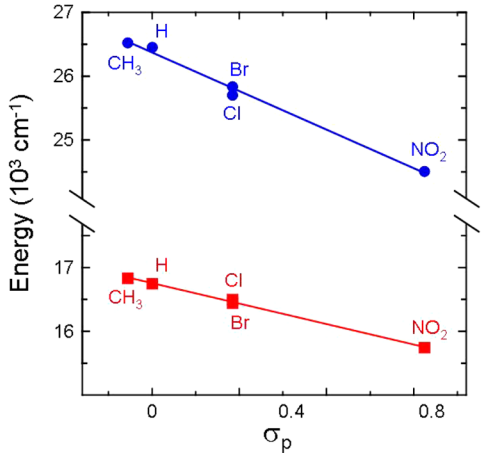

Figure 4. Plots of E_{abs} (blue circle) and E_{em} (red square) vs σ_p for **1**−**5**, where σ_p is the Hammett substituent parameter for the X substituent of the Xphen ligands. Best-fit lines: $E_{abs} = -1.2\sigma_p + 26.4$ (R, −0.99); $E_{em} = -0.6\sigma_p + 26.4$ (R, −1.00).

It is not obvious that correlations involving E_{abs} and E_{em} across d^6-electron metal ions should necessarily hold because of additional complexities, not the least of which involves solvation effects. Notwithstanding, it is apparent that, for **1**−**5**, these spectroscopic parameters are strongly correlated with the corresponding values for M(Xphen)$(CO)_4$ (M = Cr, Mo, W) across a wide range of solvents.[122−124] For example, noting that the MLCT band maximum for W(bpy)$(CO)_4$ in acetonitrile (452 nm) is nearly the same as those in DMF (454 nm) and DMSO (450 nm), it is satisfying that plots of E_{abs} for **1**−**3** and **5** versus values for W(Xphen)$(CO)_4$ in DMF and DMSO have slopes of ∼2, in accord with the relative number of Xphen ligands in the two sets of complexes (Figure S7, Supporting Information). E_{abs} and E_{em} for **1**−**3** and **5** also give linear plots ($R > 0.997$) versus values for Re(4,4′-X_2-2,2′-bipyridine)$(CO)_3$(Etpy)$^+$ (Etpy = 4-ethylpyridine) in acetonitrile (Figure S8, Supporting Information).[25] The slopes (E_{abs}, 0.50; E_{em}, 0.28) are substantially less than the ratio of the number of X substituents in the two series (i.e., 1), which is qualitatively consistent with the expected influence of two substituents on the ligand-based LUMO in the rhenium(I) series as compared to only one substituent in the Ru(Xphen)$_2$(dpte)$^{2+}$ series.

CONCLUSION

This investigation of a series of ruthenium(II) bis-diimine complexes with the π-acidic dpte thioether-donor chelate provides insight into the surprising structural, electronic, and photochemical properties of this system. Crystallized samples contained nonstatistical distributions of geometric isomers. In addition, the complexes were found to adopt rather compact geometries in the solid state, in which there are short contacts between the dpte phenyl groups and the diimine ligands. Going forward, it is anticipated that this conformational preference can be exploited to construct larger organized structures based on monomeric metal complex building blocks. The complexes also exhibit fluid solution luminescence with lifetimes in the 140−750 ns time range. This behavior stands in contrast to observations for ruthenium(II) bis-diimine complexes with π-acidic phosphine donor ligands, which typically are not luminescent in fluid solution. It would appear that, at least in the case of **8**, a low-lying d−d excited state is accessible because the complex undergoes photosubstitution reactions. Overall, the combination of promising spectroscopic, photophysical, photochemical, and electrochemical properties makes Ru(diimine)$_2$(dpte)$^{2+}$ complexes attractive candidate components for a variety of applications.

The variation in the redox potentials and MLCT state energies of the Ru(diimine)$_2$(dpte)$^{2+}$ series is consistent with the view that the diimine substituents influence the energy of the mainly diimine ligand-based LUMO to a greater extent than the energy of the mainly metal-based HOMO. The qualitative trends are by no means surprising. However, these observations sparked a closer examination than previously undertaken of the quantitative relationship between these experimental observables for a large number of complexes and summative Hammett parameters (σ_T), as well as Lever's electrochemical parameter (E_L). Variations in $E^{\circ\prime}(Ru^{3+/2+})$ due to substituents at the 4- and 7-positions of phenanthrolinyl ligands and the 4- and 4′-positions of bipyridyl ligands are decidedly more strongly correlated with σ_p^+ than σ_m or σ_p. Moreover, despite being further from the metal center, substituents at the 5- and 6-positions of phenanthrolinyl ligands exert influence on $E^{\circ\prime}(Ru^{3+/2+})$ that it is comparable to that of substituents at the 3- and 8-positions. This result is qualitatively consistent with the fact that the 5- and 6-position substituents are each within two bonds of either pyridyl ring, whereas substituents at the 3- and 8-positions only interact strongly with one ring. Overall, the rather strong relationships between $E^{\circ\prime}(Ru^{3+/2+})$, σ_T, and E_L suggest their usefulness for predicting properties and identifying unusual or suspect data. Moreover, these empirical relationships represent a benchmark against which the reliability of computational strategies for predicting properties may be evaluated.

ASSOCIATED CONTENT

Supporting Information

Crystallographic data in CIF format, bond lengths and angles, electronic spectroscopy and electrochemical data, Hammett substituent constants, E_L values, plots showing correlations involving electrochemical, and spectroscopic parameters for ruthenium and other metal complexes. This material is available free of charge via the Internet at http://pubs.acs.org.

AUTHOR INFORMATION

Corresponding Author

*E-mail: Bill.Connick@uc.edu.

Notes

The authors declare no competing financial interest.

dx.doi.org/10.1021/ic4022454 | Inorg. Chem. 2014, 53, 294−307

■ ACKNOWLEDGMENTS

This research was supported by the National Science Foundation (CHE-1152853, 0749790, 0134975). We thank Drs. Stephen Macha and Larry Sallans for expert technical assistance. N.A.F. Al-Rawashdeh thanks the Fulbright Scholar Program and the Jordan University of Science and Technology for financial support. Funding for the SMART6000 CCD diffractometer was through NSF-MRI grant CHE-0215950. Synchrotron data were collected through the SCrALS (Service Crystallography at Advanced Light Source) project at Beamline 11.3.1 at the Advanced Light Source (ALS), Lawrence Berkeley National Laboratory. The ALS is supported by the U.S. Department of Energy, Office of Energy Sciences, under contract DE-AC02-05CH11231.

■ REFERENCES

(1) Vos, J. G.; Kelly, J. M. *Dalton Trans.* **2006**, 4869−4883.
(2) Campagna, S.; Puntoriero, F.; Nastasi, F.; Bergamini, G.; Balzani, V. In *Photochemistry and Photophysics of Coordination Compounds I*; Balzani, V., Campagna, S., Eds.; Springer: Berlin, 2007; Vol. *280*, pp 117−214.
(3) Zeitler, K. *Angew. Chem., Int. Ed.* **2009**, *48*, 9785−9789.
(4) Gill, M. R.; Thomas, J. A. *Chem. Soc. Rev.* **2012**, *41*, 3179−3192.
(5) Saji, T.; Aoyagui, S. *J. Electroanal. Chem.* **1975**, *58*, 401−410.
(6) Iwamura-Kasai, M. *Nippon Kagaku Kaishi* **1983**, 1456−1462.
(7) Ohsawa, Y.; Hanck, K. W.; DeArmond, M. K. *J. Electroanal. Chem.* **1984**, *175*, 229−240.
(8) Ghosh, P.; Chakravorty, A. *Inorg. Chem.* **1984**, *23*, 2242−2248.
(9) Dodsworth, E. S.; Lever, A. B. P. *Chem. Phys. Lett.* **1984**, *112*, 567−570.
(10) Dodsworth, E. S.; Lever, A. B. P. *Chem. Phys. Lett.* **1985**, *116*, 254.
(11) Dodsworth, E. S.; Lever, A. B. P. *Chem. Phys. Lett.* **1986**, *124*, 152−158.
(12) Juris, A.; Belser, P.; Barigelletti, F.; Von Zelewsky, A.; Balzani, V. *Inorg. Chem.* **1986**, *25*, 256−259.
(13) Wacholtz, W. F.; Auerbach, R. A.; Schmehl, R. H. *Inorg. Chem.* **1986**, *25*, 227−234.
(14) Barigelletti, F.; Juris, A.; Balzani, V.; Belser, P.; A., V. Z. *Inorg. Chem.* **1987**, *26*, 4115−4119.
(15) Barqawi, K. R.; Llobet, A.; Meyer, J. T. *J. Am. Chem. Soc.* **1988**, *110*, 7751−7759.
(16) Kawanishi, Y.; Kitamura, N.; Tazuke, S. *Inorg. Chem.* **1989**, *28*, 2968−2975.
(17) Greaney, M. A.; Coyle, C. L.; Harmer, M. A.; Jordan, A.; Stiefel, E. I. *Inorg. Chem.* **1989**, *28*, 912−920.
(18) Ciana, L. D.; Dressick, W. J.; Sandrini, D.; Maestri, M.; Ciano, M. *Inorg. Chem.* **1990**, *29*, 2792−2798.
(19) Vlcek, A. A.; Dodsworth, E. S.; Pietro, W. J.; Lever, A. B. P. *Inorg. Chem.* **1995**, *34*, 1906−1913.
(20) Maestri, M.; Armaroli, N.; Balzani, V.; Constable, E. C.; Thompson, A. M. W. C. *Inorg. Chem.* **1995**, *34*, 2759−2767.
(21) Murali, M.; Palaniandavar, M. *Dalton Trans.* **2006**, 730−743.
(22) Murali, M.; Palaniandavar, M. *Polyhedron* **2007**, *26*, 3980−3992.
(23) Johnson, S. R.; Westmoreland, T. D.; Caspar, J. V.; Barqawi, K. R.; Meyer, T. J. *Inorg. Chem.* **1988**, *27*, 3195−3200.
(24) Juris, A.; Campagna, S.; Bidd, I.; Lehn, J. M.; Ziessel, R. *Inorg. Chem.* **1988**, *27*, 4007−4011.
(25) Hino, J. K.; Ciana, L. D.; Dressick, W. J.; Sullivan, B. P. *Inorg. Chem.* **1992**, *31*, 1072−1080.
(26) Wallace, L.; Rillema, D. P. *Inorg. Chem.* **1993**, *32*, 3836−3843.
(27) Cummings, S. D.; Eisenberg, R. *J. Am. Chem. Soc.* **1996**, *118*, 1949−1960.
(28) Batista, A. A.; Santiago, M. O.; Donnici, C. L.; Moreira, I. S.; Healy, P. C.; Berners-Price, S. J.; Queiroz, S. L. *Polyhedron* **2001**, *20*, 2123−2128.
(29) Elliott, C. M.; Hershenhart, E. J. *J. Am. Chem. Soc.* **1982**, *104*, 7519−7526.
(30) Schott, E.; Zarate, X.; Arratia-Perez, R. *J. Phys. Chem. A* **2012**, *116*, 7436−7442.
(31) Konezny, S. J.; Doherty, M. D.; Luca, O. R.; Crabtree, R. H.; Soloveichik, G. L.; Batista, V. S. *J. Phys. Chem. C* **2012**, *116*, 6349−6356.
(32) Mukherjee, R.; Chakravorty, A. *J. Chem. Soc., Dalton Trans.* **1983**, 2197−2203.
(33) Guarr, T. F.; Anson, F. C. *J. Phys. Chem.* **1987**, *91*, 4037−4043.
(34) Baitalik, S.; Adhikary, B. *Polyhedron* **1997**, *16*, 4073−4080.
(35) Das, C.; Kamar, K. K.; Ghosh, A. K.; Majumdar, P.; Hung, C.-H.; Goswami, S. *New J. Chem.* **2002**, *26*, 1409−1414.
(36) Le Lagadec, R.; Rubio, L.; Alexandrova, L.; Toscano, R. A.; Ivanova, E. V.; Meškys, R.; Laurinavièius, V.; Pfeffer, M.; Ryabov, A. D. *J. Organomet. Chem.* **2004**, *689*, 4820−4832.
(37) Skarda, V.; Cook, M. J.; Lewis, A. P.; McAuliffe, G. S. G.; Thomson, A. J.; Robbins, D. J. *J. Chem. Soc., Perkins 2* **1984**, 1309−1311.
(38) Nazeeruddin, M. K.; Zakeeruddin, S. M.; Kalyanasundaram, K. *J. Phys. Chem.* **1993**, *97*, 9607−9612.
(39) Masui, H.; Lever, A. B. P. *Inorg. Chem.* **1993**, *32*, 2199−2201.
(40) Pichot, F.; Beck, J. H.; Elliott, C. M. *J. Phys. Chem. A* **1999**, *103*, 6263−6267.
(41) Geißer, B.; Skrivanek, T.; Zimmermann, U.; Stufkens, D. J.; Alsfasser, R. *Eur. J. Inorg. Chem.* **2001**, *2001*, 439−448.
(42) Taylor, P. J.; Schilt, A. A. *Inorg. Chim. Acta* **1971**, *5*, 691−697.
(43) Haga, M.-a.; Matsumura-Inoue, T.; Shimizu, K.; Sato, G. P. *J. Chem. Soc., Dalton Trans.* **1989**, *0*, 371−373.
(44) Lever, A. B. P. *Inorg. Chem.* **1990**, *29*, 1271−1285.
(45) Xiao, X.; Sakamoto, J.; Tanabe, M.; Yamazaki, S.; Yamabe, S.; Takeko, M.-I. *J. Electroanal. Chem.* **2002**, *527*, 33−40.
(46) Lever, A. B. P. In *Comprehensive Coordination Chemistry, II*; Lever, A. B. P., Ed.; Elsevier Science: Boston, 2004; Vol. *2*, pp 251−268.
(47) McClanahan, S. F.; Dallinger, R. F.; Holler, F. J.; Kincaid, J. R. *J. Am. Chem. Soc.* **1985**, *107*, 4853−4860.
(48) Mabrouk, P. A.; Wrighton, M. S. *Inorg. Chem.* **1986**, *25*, 526−531.
(49) Damrauer, N. H.; Boussie, T. R.; Devenney, M.; McCusker, J. K. *J. Am. Chem. Soc.* **1997**, *119*, 8253−8268.
(50) Curtright, A. E.; McCusker, J. K. *J. Phys. Chem. A* **1999**, *103*, 7032−7041.
(51) Benniston, A. C.; Harriman, A.; Romero, F. M.; Ziessel, R. *Dalton Trans.* **2004**, *0*, 1233−1238.
(52) Alford, P. C.; Cook, M. J.; Lewis, A. P.; McAuliffe, G. S. G.; Skarda, V.; Thomson, A. J. *J. Chem. Soc., Perkins Trans. 2* **1985**, 705−709.
(53) Brunschwig, B.; Sutin, N. *J. Am. Chem. Soc.* **1978**, *100*, 7568−7577.
(54) Yan, S. G.; Prieskorn, J. S.; Kim, Y.; Hupp, J. T. *J. Phys. Chem. B* **2000**, *104*, 10871−10877.
(55) Shinozaki, K.; Shinoyama, T. *Chem. Phys. Lett.* **2006**, *417*, 111−115.
(56) O'Neill, L.; Perdisatt, L.; O'Connor, C. *J. Phys. Chem. A* **2012**, *116*, 10728−10735.
(57) Ye, B.-H.; Ji, L.-N.; Xue, F.; Mak, T. W. *Transition Met. Chem.* **1999**, *24*, 8−12.
(58) Bare, W. D.; Mack, N. H.; Demas, J. N.; DeGraff, B. A. *Appl. Spectrosc.* **2004**, *58*, 1093−1100.
(59) Dragonetti, C.; Falciola, L.; Mussini, P.; Righetto, S.; Roberto, D.; Ugo, R.; Valore, A.; De Angelis, F.; Fantacci, S.; Sgamellotti, A.; Ramon, M.; Muccini, M. *Inorg. Chem.* **2007**, *46*, 8533−8547.
(60) Root, M. J.; Sullivan, B. P.; Meyer, T. J.; Deutsch, E. *Inorg. Chem.* **1985**, *24*, 2731−2739.
(61) Collin, J.-P.; Jouvenot, D.; Koizumi, M.; Sauvage, J. P. *Inorg. Chim. Acta* **2007**, *360*, 923−930.
(62) Sahawakfeh, K. Q.; Al-Rawashdeh, N. A. F.; Khader, S. *Russ. J. Coord. Chem.* **2002**, *28*, 841.

(63) Hissler, M.; Connick, W. B.; Geiger, D. K.; McGarrah, J. E.; Lipa, D.; Lachicotte, R. J.; Eisenberg, R. *Inorg. Chem.* **2000**, *39*, 447−457.
(64) Curtis, J. C.; Bernstein, J. S.; Meyer, T. J. *Inorg. Chem.* **1985**, *24*, 385−397.
(65) Sawyer, D. T.; Roberts, J. L. *Experimental Electrochemistry for Chemists*; John-Wiley: New York, 1974.
(66) Pavlishchuk, V. V.; Addison, A. W. *Inorg. Chim. Acta* **2000**, *298*, 97−102.
(67) Zar, R. H. *Biostatistical Analysis*; Prentice Hall: Upper Saddle River, NJ, 1999.
(68) Steiger, J. H. *Psychol. Bull.* **1980**, *87*, 245−251.
(69) Juris, A.; Balzani, V.; Barigelletti, F.; Campagna, S.; Belser, P.; von Zelewsky, A. *Coord. Chem. Rev.* **1988**, *84*, 85−277.
(70) Hansch, C.; Leo, A.; Hoekman, D. *Exploring QSAR: Hydrophobic, Electronic, and Steric Constants*; American Chemical Society: Washington DC, 1995.
(71) Meites, L. *Handbook of Analytical Chemistry*, 1st ed.; McGraw-Hill: New York, 1963.
(72) Bard, A. J.; Faulkner, L. R. *Electrochemical Methods: Fundamentals and Applications*, 2nd ed.; John Wiley & Sons, Inc.: New York, 2001.
(73) Juris, A.; Barigelletti, F.; Balzani, V.; Belser, P.; von Zelewsky, A. *Israel J. Chem.* **1982**, *22*, 87−90.
(74) Sullivan, B. P.; Salmon, D. J.; Meyer, T. J. *Inorg. Chem.* **1978**, *17*, 3334−3341.
(75) Giordano, P. J.; Bock, C. R.; Wrighton, M. S. *J. Am. Chem. Soc.* **1978**, *100*, 6960−6965.
(76) (a) *APEX2*, v2.1−4; *SMART*, v5.632; and *SAINT* v6.45A, v7.34A; Bruker AXS, Inc.: Madison, WI. (b) Sheldrick, G. M. *SADABS*, v2.10, v2004/1, v2008/1; University of Göttingen: Göttingen, Germany. (c) SIR2004 v1.0. Giacovazzo, C.; et al. *J. Appl. Crystallogr.* **2004**, *37*, 258−791. (d) Sheldrick, G. M. *SHELXTL*, v6.14; Bruker AXS, Inc.; Madison, WI, 2000. (e) Brandenburg, K. *Diamond*, v3.2c; Crystal Impact: Bonn, Germany.
(77) McDevitt, M. R.; Ru, Y.; Addison, A. W. *Trans. Met. Chem.* **1993**, *18*, 197−204.
(78) Kvam, P.-I.; Songstad, J. *Acta Chem. Scand.* **1995**, *49*, 313−324.
(79) Aydin, N.; Schlaepfer, C.-W. *Polyhedron* **2000**, *20*, 37−45.
(80) Cross, R. J.; Dalgleish, I. G.; Smith, G. J.; Wardle, R. *J. Chem. Soc., Dalton Trans.* **1972**, 992−996.
(81) Hartley, F. R.; Murray, S. G.; Levason, W.; Soutter, H. E.; McAuliffe, C. A. *Inorg. Chim. Acta* **1979**, *35*, 265−277.
(82) Gulliver, D. J.; Levason, W.; Smith, K. G.; Selwood, M. J.; Murray, S. G. *J. Chem. Soc., Dalton Trans.* **1980**, 1872−1878.
(83) Durham, B.; Caspar, J. V.; Nagle, J. K.; Meyer, J. M. *J. Am. Chem. Soc.* **1982**, *104*, 4803−4810.
(84) Baranoff, E.; Collin, J.-P.; Furusho, J.; Furusho, Y.; Laemmel, A.-C.; Sauvage, J.-P. *Inorg. Chem.* **2002**, *41*, 1215−1222.
(85) de Silva, A. P.; Gunarate, H. Q. N.; Gunnlaugsson, T.; Huxley, A. J. M.; McCoy, P.; Rademacher, J. D.; Rice, T. E. *Chem. Rev.* **1997**, *97*, 1515−2433.
(86) Works, C. F.; Jocher, C. J.; Bart, G. D.; Bu, X.; Fort, P. C. *Inorg. Chem.* **2002**, *41*, 3728−3739.
(87) Orpen, A. G.; Brammer, L.; Allen, F. H.; Kennard, O.; Watson, D. G.; Taylor, R. *J. Chem. Soc., Dalton Trans.* **1989**, S1.
(88) Shaver, A.; Plouffe, P. Y. *J. Am. Chem. Soc.* **1991**, *113*, 7780−7782.
(89) Zhiqina, J.; Huang, S. D.; Guadalupe, A. R. *Inorg. Chim. Acta* **2000**, *305*, 127−134.
(90) Yea, B.-H.; Chena, X.-M.; Zenga, T.-X.; Jia, L.-N. *Inorg. Chim. Acta* **1995**, *240*, 5−11.
(91) Comba, P.; Fath, A.; Hambley, T. W.; Kuhner, A.; Richens, D. T.; Vielfort, A. *Inorg. Chem.* **1998**, *37*, 4389−4401.
(92) Pinxi, S.; Xinkan, Y.; Yixing, G. *Huaxue Xuebao* **1984**, *42*, 20.
(93) Marangoni, G.; Pitteri, B.; Bertolasi, V.; Gilli, P. *Inorg. Chim. Acta* **1995**, *234*, 173−179.
(94) Bautista, J.; Bertran, A.; Bernes, S.; Duran, U.; Torrens, H. *Rev. Soc. Quim. Mex.* **2003**, *47*, 44−52.
(95) Sauvage, J. P.; Collin, J. P.; Chambron, J. C.; Guillerez, S.; Coudret, C.; Balzani, V.; Barigelletti, F.; de Cola, L.; Flamigni, L. *Chem. Rev.* **1994**, *94*, 993−1019.
(96) Rillema, D. P.; Allan, G.; Meyer, T. J.; Conrad, D. *Inorg. Chem.* **1983**, *22*, 1617−1622.
(97) Callahan, R. W.; Keene, F. R.; Meyer, T. J.; Salmon, D. J. *J. Am. Chem. Soc.* **1977**, *99*, 1064−1073.
(98) Carlin, C. M.; de Armond, M. K. *Chem. Phys. Lett.* **1982**, *89*, 297−302.
(99) Maki, A. H.; Geske, D. H. *J. Am. Chem. Soc.* **1961**, *83*, 1852−1860.
(100) Bracco, L. L. B. Ñ.; Lezna, R. O.; Muñoz-Zuñiga, J.; Ruiz, G. T.; Féliz, M. R.; Ferraudi, G. J.; García Einschlag, F. S.; Wolcan, E. *Inorg. Chim. Acta* **2011**, *370*, 482−491.
(101) Matsumura-Inoue, T.; Ikemoto, I.; Umezawa, Y. *J. Electroanal. Chem.* **1986**, *209*, 135−150.
(102) Cooper, S. R.; Rawle, S. C. *Struc. Bond.* **1992**, *72*, 1−72.
(103) Thomas, J. A. *Coord. Chem. Rev.* **2013**, *257*, 1555−1563.
(104) de Armond, M. K.; Carlin, C. M.; Huang, W. L. *Inorg. Chem.* **1980**, *19*, 62−67.
(105) Miskowski, V. M.; Houlding, V. H. *Inorg. Chem.* **1989**, *28*, 1529−1533.
(106) Bray, R. G.; Ferguson, J.; Hawkins, C. J. *Aust. J. Chem.* **1969**, *22*, 2091−2103.
(107) Connick, W. B.; Miskowski, V. M.; Houlding, V. H.; Gray, H. B. *Inorg. Chem.* **2000**, *39*, 2585−2592.
(108) Green, T. W.; Lieberman, R.; Mitchell, N.; Krause Bauer, J. A.; Connick, W. B. *Inorg. Chem.* **2005**, *44*, 1955−1965.
(109) Basu, A.; Weiner, M. A.; Strekas, T. C.; Gafney, H. D. *Inorg. Chem.* **1982**, *21*, 1085−1092.
(110) Myrick, M. L.; Armond, M. K. *J. Phys. Chem.* **1989**, *93*, 7099.
(111) Myrick, M. L.; Blakley, R. L.; De Armond, M. K. *J. Phys. Chem.* **1989**, *93*, 3936−3940.
(112) Suzuki, T.; Kuchiyama, T.; Kishi, S.; Kaizaki, S.; Kato, M. *Bull. Chem. Soc. Jpn.* **2002**, *75*, 2433−2439.
(113) Gabrielsson, A.; Matousek, P.; Towrie, M.; Hartl, F. e.; Záliš, S.; Vlèek, A. *J. Phys. Chem. A* **2005**, *109*, 6147−6153.
(114) Klein, A.; Kaim, W.; Waldhor, E.; Hausen, H. D. *J. Chem. Soc., Perkins Trans. 2* **1995**, 2121−2126.
(115) Ernst, S.; Vogler, C.; Klein, A.; Kaim, W.; Zališ, S. *Inorg. Chem.* **1996**, *35*, 1295−1300.
(116) Farrell, I. R.; Hartl, F.; Záliš, S.; Mahabiersing, T.; Vlcek, A. J. *J. Chem. Soc., Dalton Trans.* **2000**, *2000*, 4323−4331.
(117) Because the 5,6-position substituents on the phenanthrolinyl ligand are one bond further from the metal than substituents at the 3,8-positions, we explored usage of an additional multiplicative factor for $\sigma(4,7)$ in σ_T in eq 2. Unfortunately, the data sets discussed here are too limited for rigorous testing of this hypothesis, and improvements in the fits were not statistically significant.
(118) If a single, high leverage data point (i.e., 4,7-dihydroxy-1,10-phenanthroline) is excluded, then the correlation with $\sigma_T[\sigma_m;\sigma_p^+;\sigma_m]$ (R, 0.909) is slightly stronger than that with $\sigma_T[\sigma_m;\sigma_p^+;\sigma_m]$ (R, 0.890).
(119) Bush, P. M.; Whitehead, J. P.; Pink, C. C.; Gramm, E. C.; Eglin, J. L.; Watton, S. P.; Pence, L. E. *Inorg. Chem.* **2001**, *40*, 1871−1877.
(120) Brodovitch, J. C.; Haines, R. I.; McAuley, A. *Can. J. Chem.* **1981**, *59*, 1610.
(121) Lin, C. T.; Boettcher, W.; Chou, M.; Creutz, C.; Sutin, N. *J. Am. Chem. Soc.* **1976**, *98*, 6536−6544.
(122) Wrighton, M. S.; Morse, D. L. *J. Organomet. Chem.* **1975**, *97*, 405−419.
(123) Manuta, D. M.; Lees, A. J. *Inorg. Chem.* **1983**, *22*, 3825−3828.
(124) Manuta, D. M.; Lees, A. J. *Inorg. Chem.* **1986**, *25*, 1354−1359.